International Journal of Solids and Structures 46 (2009) 4451–4477

Contents lists available at ScienceDirect

International Journal of Solids and Structures

journal homepage: www.elsevier.com/locate/ijsolstr

A numerical study on the solution of the Cauchy problem in elasticity

Antonio Bilotta [a], Emilio Turco [b,*]

[a] Dipartimento di Modellistica per l'Ingegneria, Università della, Calabria, Rende (CS), Italy
[b] DAP, Università degli Studi di Sassari, Alghero (SS), Italy

ARTICLE INFO

Article history:
Received 6 June 2009
Received in revised form 24 August 2009
Available online 13 September 2009

Keywords:
Inverse problems
Cauchy problems
Regularization techniques

ABSTRACT

This work deals with the Cauchy problem in two-dimensional linear elasticity. The equations of the problem are discretized through a standard FEM approach and the resulting ill-conditioned discrete problem is solved within the frame of the Tikhonov approach, the choice of the required regularization parameter is accomplished through the Generalized Cross Validation criterion. On this basis a numerical experimentation has been performed and the calculated solutions have been used to highlight the sensitivity to the amount of known data, the noise always present in the data, the regularity of boundary conditions and the choice of the regularization parameter. The aim of the numerical study is to implicitly device some guidelines to be used in the solution of this kind of problems.

1. Introduction

Inverse problems in elasticity is becoming an important emerging field whose engineering applications, following Bonnet and Constantinescu (2005), can be grouped as follows:

- reconstruction of buried objects such as cracks, cavities and inclusions or residual stresses;
- identification of constitutive properties also used in model updating;
- identification of inaccessible boundary values (Cauchy problem).

The present work is devoted to the solution of Cauchy problem in linear elasticity which can be formulated as follows: given the tractions and displacements on the accessible part of the boundary of an elastic body, to evaluate the same information on the inaccessible part of the boundary. This problem has many practical applications since in actual problems sometimes the data are not complete. Moreover the same problem has to be solved, as a preliminary step, also in the identification of buried objects. In this case, following the approach presented for elastic bodies in Alessandrini et al. (2003) from a theoretical point of view and in Alessandrini et al. (2005) in a numerical contest, a complete knowledge of the traction and displacement fields along the boundary is required.

Due to the severity of the ill-posedness of the Cauchy problem, see Belgacem (2007) for example, several solution methods were proposed, as testified by the rich literature on the matter. They can approximatively be grouped as follows.

1. The quasi-reversibility method introduced in Lattès and Lions (1967) and used in the solution of the Laplace problem by using the finite difference method in Klibanov and Santosa (1991) and the mixed finite element method in Bourgeois (2005).
2. Iterative methods such as that presented in Kozlov et al. (1991) and used in the framework of the boundary element method to solve the Laplace equation, in Lesnic et al. (1997) and Jourhmane et al. (2004), Helmholtz equation, in Marin et al. (2003a), stationary Stokes system, in Bastay et al. (2006), and linear elastic problems, in Marin et al. (2001, 2002a) and Comino et al. (2007). In Lesnic et al. (1997) the problem of the convergence criterion is also considered and in order to improve the convergence rate a relaxation procedure is experimented in Jourhmane et al. (2004) and Marin et al. (2001). The conjugate gradient strategy is used in Hào and Lesnic (2000) and Bastay et al. (2001) for the Laplace equation, in Marin et al. (2002b) for elasticity, in Marin et al. (2003b) for Helmholtz-type equation and, finally, in Johansson and Lesnic (2006a) for determining the fluid velocity of a slow viscous flow. A variant of the conjugate gradient strategy, namely the Minimal Error Method, is used in Johansson and Lesnic (2006b) for the reconstruction of a stationary flow, in Marin (2009a) in the field of linear elasticity and in Marin (2009b) for Helmholtz-type equations. Finally, the Landweber–Fridman iterative method is used in Marin et al. (2004a) for Helmholtz-type equation, in Marin and Lesnic (2005) for linear elasticity and in Johansson and Lesnic (2007) for the reconstruction of a stationary flow.
3. Methods based on the minimization of an energy-like functional as proposed in Andrieux et al. (2006) for solving the Laplace equation and in Andrieux and Baranger (2008) for the analysis of elastic systems.

* Corresponding author. Tel.: +39 9720403; fax: +39 9720420.
E-mail address: emilio.turco@uniss.it (E. Turco).

0020-7683/$ - see front matter © 2009 Elsevier Ltd. All rights reserved.
doi:10.1016/j.ijsolstr.2009.09.006

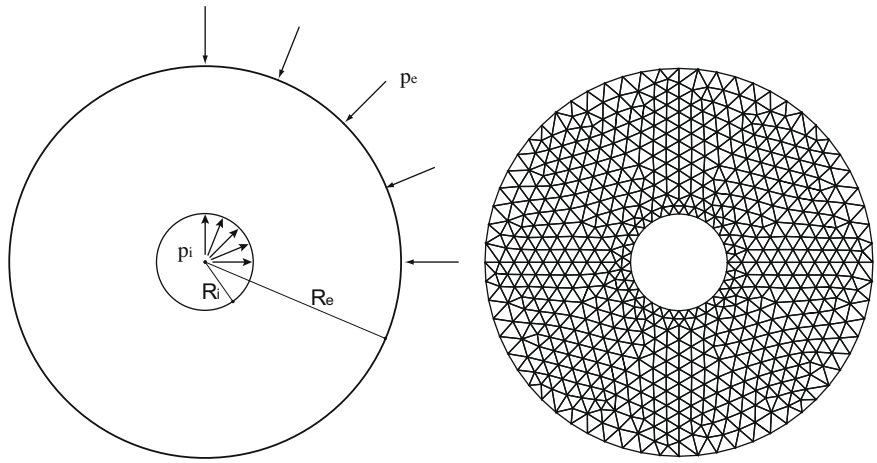

Fig. 1. Hollow cylinder under pressure test: geometry, load condition and finite element discretization.

Table 1
Meshes used for the analysis of the hollow cylinder.

Thin	*Medium*	*Thick*
64 × 64 × 2	32 × 48 × 5	32 × 64 × 10
96 × 96 × 3	64 × 96 × 10	64 × 128 × 20
128 × 128 × 4	128 × 192 × 20	96 × 192 × 30
256 × 256 × 8		

4. Methods based on the Tikhonov regularization (Tikhonov and Arsenin, 1977) have been adopted in several contributions. Among them we cite Cimetière et al. (2001) where the steady state heat equation is solved through an iterative strategy which allows to avoid the selection of the regularization parameter. In Marin and Lesnic (2002a) the elastic problem is solved by using boundary elements and the criterion used to choose the optimal solution is based on the discrepancy principle coded in the Singular Value Decomposition. In Marin and Lesnic (2002b) the optimal solution is selected by the *L*-curve criterion. Marin and Lesnic (2003), again in the analysis of the elastic problem by the boundary element method, identifies unknown portions of the boundary by using the *L*-curve method as criterion for selecting the regularization parameter and Marin et al. (2004b) presents the comparison of various regularization methods for solving problem associated with Helmholtz equation.

Finally, in order to cite also some contributions which do not fit the previous classification, in Burke et al. (2007) the identification of residual stress field in an elastic body is obtained through a partial polar decomposition, a sort of regularization similar to truncated Singular Value Decomposition, based on a spectral decomposition. Marin and Lesnic (2004), Marin (2005) and Wang et al. (2006) use the method of fundamental solutions to build a meshless strategy. Contributions (Yeih et al., 1993; Koya et al., 1993) can be framed into the so-called ficticious boundary indirect method, the first contribution proposes the theoretical approach and the second one issues some numerical details. Other interesting contributions are represented by Maniatty et al. (1989), Zabaras et al. (1989) and Schnur and Zabaras (1990). Contribution (Maniatty et al., 1989) proposes a simple diagonal regularization to determine boundary tractions using the finite element method. The concept of the spatial regularization is adopted in the frame of the boundary element method in Zabaras et al. (1989) and of the finite element method in Schnur and Zabaras (1990). Other papers use auxiliary data to recover boundary conditions. For example Maniatty and Zabaras (1994) uses the internal displacement field while Turco (1998, 1999, 2001) use the internal stress or strain fields.

The aim of the present work is to present a qualitative and quantitative study on the solution of the Cauchy problem in linear elasticity. The study is performed analyzing two-dimensional elastic problems by a standard FEM discretization. The discrete ill-posed problem derived through the discretization is tackled with the Singular Value Decomposition (Golub and Van Loan, 1996) of the problem matrix and the searched solution is calculated on the basis of a Tikhonov regularization (Tikhonov and Arsenin, 1977) of the problem.

Roughly speaking, this approach perturbs the singular values of the system matrix shifting them by an unknown parameter which plays a fundamental role in the solution of the system. The parameter, called the *regularization parameter*, makes possible to evaluate a solution of the problem and filter out the noise always present in the data. Its selection must be performed by using an external criterion, the Generalized Cross Validation (Golub et al., 1979) criterion has been adopted in the present work.

The described numerical approach has been used to study the sensitivity of the obtained solution with respect to some factors: the ratio between the length of the accessible part of the boundary and the length of the inaccessible part of the boundary, *i.e.* the amount of Cauchy data that can be used to solve the problem; the errors contained in the known boundary data; the presence of discontinuities in the domain of the problem to be solved and in the boundary conditions to be reconstructed; the chosen regularization parameter. The main aim of this numerical experimentation is to devise some guidelines useful in the solution of this kind of problems.

The paper is organized as follows. Next section describes the formulation of Cauchy problem in linear elasticity and its discretization through a standard finite element approach. Section 3 discusses the algorithm used to reconstruct the unknown boundary values. Several numerical results are presented and discussed in Section 4 and, finally, some concluding remarks, reported in Section 5, close the paper.

2. Problem keynotes

Let us consider a generic elastic body $\mathscr{B}$ loaded by the bulk force $\mathbf{f}$ and the traction $\mathbf{t}$ on the boundary $\partial\mathscr{B}$. The associated potential energy functional can be formulated as follows:

$$J := \frac{1}{2}\int_{\mathscr{B}} (\mathbf{Dd})^{\mathrm{T}}\mathbf{EDd}\,\mathrm{d}V - \int_{\mathscr{B}} \mathbf{d}^{\mathrm{T}}\mathbf{f}\,\mathrm{d}V - \int_{\partial\mathscr{B}} \mathbf{d}^{\mathrm{T}}\mathbf{t}\,\mathrm{d}S. \tag{2.1}$$

In the latter equation, following a standard notation in finite elements literature (Zienkiewicz and Taylor, 2000), **d** is a vector collecting the components of the displacement field, **D** is the operator which transforms components of displacement into components of strain and **E** is the elastic constitutive matrix.

The derivation of the finite element model from (2.1) requires the subdivision of the domain into non-overlapping finite elements and the interpolation, at the element level, of the unknown displacement field

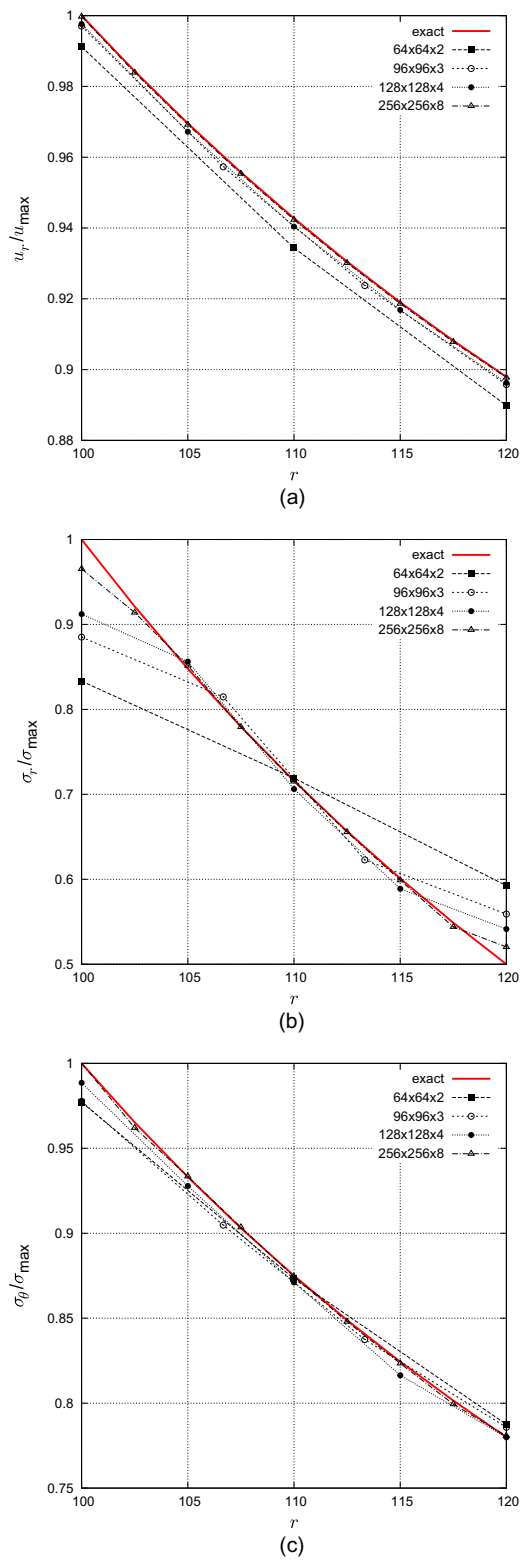

Fig. 2. Thin hollow cylinder under pressure: comparison between analytical and numerical solution of the direct problem varying the mesh (u_r, (a), σ_r, (b), and σ_θ, (c), along the radius).

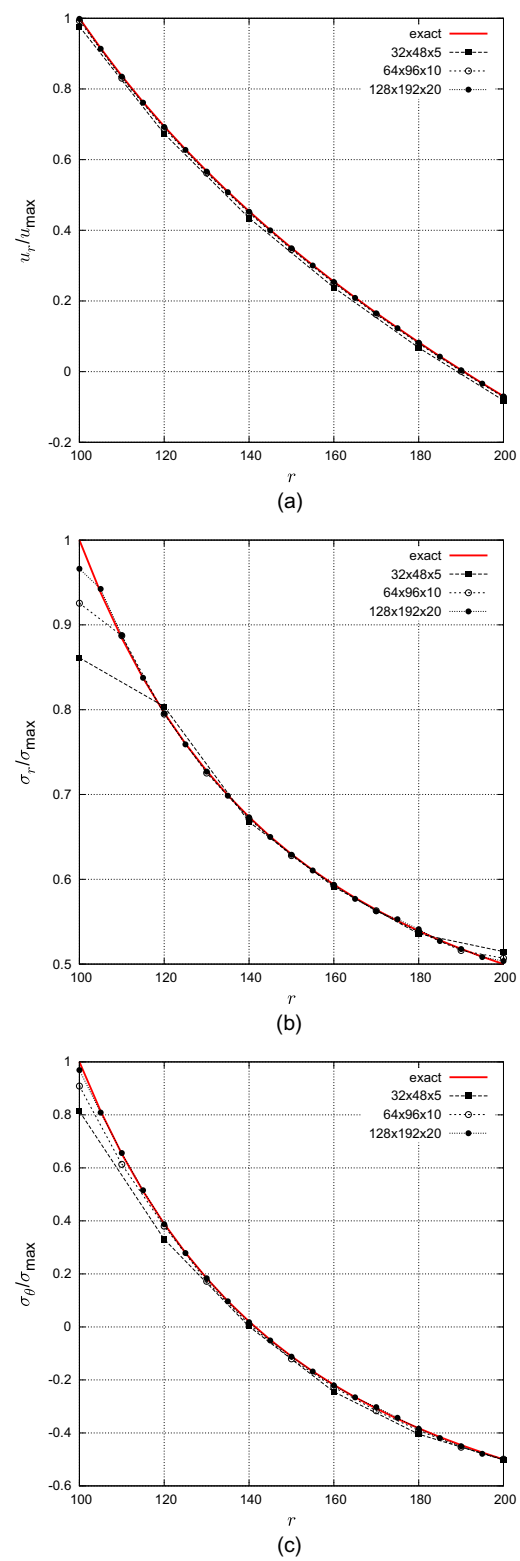

Fig. 3. *Medium* hollow cylinder under pressure: comparison between analytical and numerical solution of the direct problem varying the mesh (u_r, (a), σ_r, (b), and σ_θ, (c), along the radius).

$$\mathbf{d} \approx \mathbf{N}\mathbf{w}_e, \tag{2.2}$$

whose only requirement is the $\mathscr{C}^0$ continuity inside and between the elements of the mesh. In (2.2) $\mathbf{N}$ is the matrix containing the interpolating fields and $\mathbf{w}_e$ is the vector collecting the discrete parameters relative to a generic element of the mesh. The finite element formulation of the potential energy functional now becomes

$$J \approx \sum_e \left(\frac{1}{2} \int_{\mathscr{B}_e} (\mathbf{D}\mathbf{N}\mathbf{w}_e)^{\mathrm{T}} \mathbf{E}\mathbf{D}\mathbf{N}\mathbf{w}_e \mathrm{d}V - \int_{\mathscr{B}_e} (\mathbf{N}\mathbf{w}_e)^{\mathrm{T}} \mathbf{f} \mathrm{d}V - \int_{\partial\mathscr{B}_e} (\mathbf{N}\mathbf{w}_e)^{\mathrm{T}} \mathbf{t} \mathrm{d}S \right), \tag{2.3}$$

or, in a more concise form,

$$J \approx \sum_e \left(\frac{1}{2} \mathbf{w}_e^{\mathrm{T}} \mathbf{K}_e \mathbf{w}_e - \mathbf{w}_e^{\mathrm{T}} \mathbf{p}_e \right), \tag{2.4}$$

where

$$\mathbf{K}_e = \int_{\mathscr{B}_e} (\mathbf{D}\mathbf{N})^{\mathrm{T}} \mathbf{E}\mathbf{D}\mathbf{N} \mathrm{d}V, \quad \mathbf{p}_e = \int_{\mathscr{B}_e} \mathbf{N}^{\mathrm{T}} \mathbf{f} \mathrm{d}V + \int_{\partial\mathscr{B}_e} \mathbf{N}^{\mathrm{T}} \mathbf{t} \mathrm{d}S, \tag{2.5}$$

represent the stiffness matrix and the load vector of the generic element of the mesh. The stationary condition of the functional (2.4) gives the following linear discrete problem:

$$\mathbf{K}\mathbf{w} = \mathbf{p}. \tag{2.6}$$

In the latter equation the quantities $\mathbf{K}, \mathbf{w}$ and $\mathbf{p}$ refer to the global problem and are obtained by a standard assemblage of all contribution of the elements.

Now, from the discrete formulation (2.6), let us derive an inverse statement of the same problem also known in the literature as Cauchy problem. Let us consider the same linear elastic body $\mathscr{B}$ and suppose that its boundary is divided into three parts $\partial\mathscr{B}_d, \partial\mathscr{B}_o$ and $\partial\mathscr{B}_u$ such that $\partial\mathscr{B} = \partial\mathscr{B}_d \cup \partial\mathscr{B}_o \cup \partial\mathscr{B}_u$. The three parts of the boundary have the following meanings.

1. $\partial\mathscr{B}_d$ is the part of the boundary where the known boundary conditions are sufficient to make the elasto-static problem well-posed in the Hadamard sense, the index d stands for determined. In other words this is the part of the boundary where it is possible to have Dirichlet, or Neumann, or mixed boundary or Robin boundary conditions.
2. $\partial\mathscr{B}_o$ is the part of the boundary where the known boundary conditions are more than those strictly sufficient to make well-posed the problem, the index o stands for overdetermined, and it represents usually the accessible part of the boundary;
3. $\partial\mathscr{B}_u$ is the part of the boundary where the known boundary conditions are less than those strictly sufficient to make well-posed the problem, the index u stands for underdetermined, and it represents usually the inaccessible part of the boundary.

This partition of the boundary can be reflected in the formulation of the discrete problem by a suitable reordering of the variables collected in the displacement vector $\mathbf{w}$ and the load vector $\mathbf{p}$, *i.e.*:

$$\mathbf{w} = \begin{bmatrix} \mathbf{w}_u \\ \mathbf{w}_d \\ \mathbf{w}_i \\ \mathbf{w}_o \end{bmatrix}, \quad \mathbf{p} = \begin{bmatrix} \mathbf{p}_u \\ \mathbf{p}_d \\ \mathbf{p}_i \\ \mathbf{p}_o \end{bmatrix}, \tag{2.7}$$

where in addition to the indexes already introduced, the index i is used to label the degrees of freedom associated to the nodes internal to the domain.

Following the notation just introduced and assuming, without loss of generality but only to make simpler the exposition, Neumann boundary conditions on $\partial\mathscr{B}_d$, the equilibrium equation (2.6) can be rewritten in the form (2.8) where only the subvectors $\mathbf{w}_u, \mathbf{w}_d$ and $\mathbf{p}_u$ have to be regarded as unknowns (the index i has been deleted counting the relative degrees of freedom among the

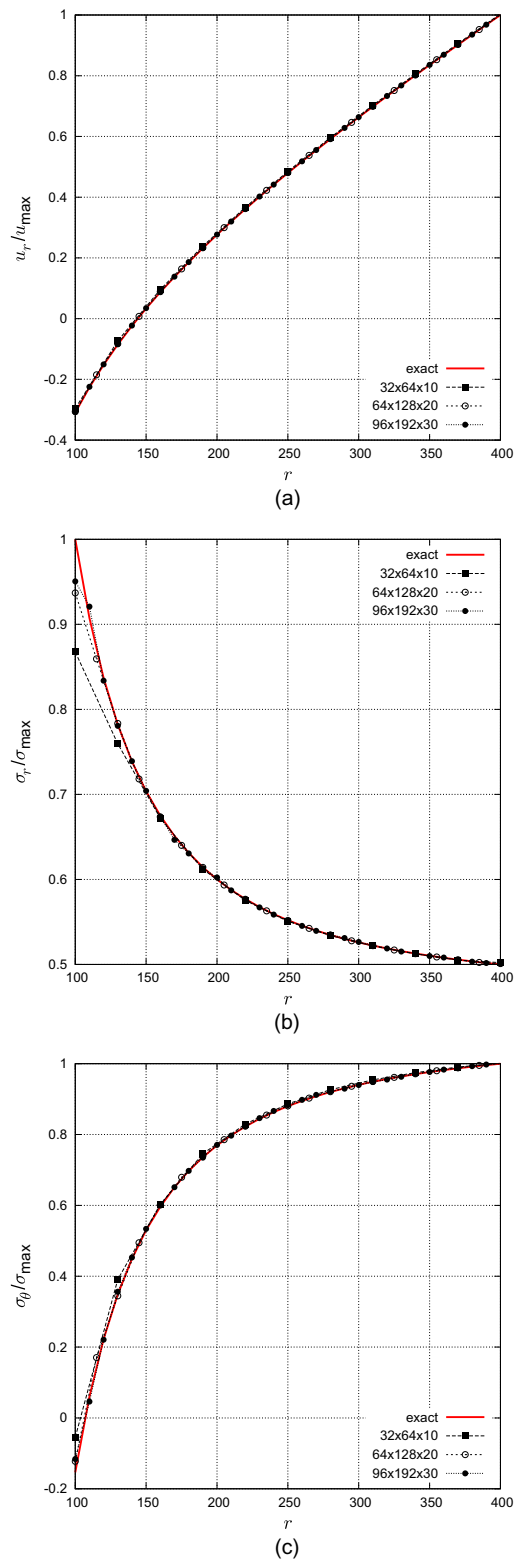

Fig. 4. *Thick* hollow cylinder under pressure: comparison between analytical and numerical solution of the direct problem varying the mesh (u_r, (a), σ_r, (b), and σ_θ, (c), along the radius).

determined ones). In this way, the equilibrium Eqs. (2.6) can be rewritten in the form

$$\begin{bmatrix} \mathbf{K}_{uu} & \mathbf{K}_{ud} & \mathbf{K}_{uo} \\ \mathbf{K}_{du} & \mathbf{K}_{dd} & \mathbf{K}_{do} \\ \mathbf{K}_{ou} & \mathbf{K}_{od} & \mathbf{K}_{oo} \end{bmatrix} \begin{bmatrix} \mathbf{w}_u \\ \mathbf{w}_d \\ \mathbf{w}_o \end{bmatrix} = \begin{bmatrix} \mathbf{p}_u \\ \mathbf{p}_d \\ \mathbf{p}_o \end{bmatrix}, \tag{2.8}$$

where only the subvectors $\mathbf{w}_u, \mathbf{w}_d$ and $\mathbf{p}_u$ have to be regarded as unknowns. We stress that the submatrices $\mathbf{K}_{uu}, \ldots, \mathbf{K}_{oo}$ are simply defined by the rearrangement of the stiffness matrix $\mathbf{K}$ which follows that of subvectors $\mathbf{w}_u, \mathbf{w}_d$ and $\mathbf{p}_u$.

As a consequence the system can be rearranged for the solution as follows:

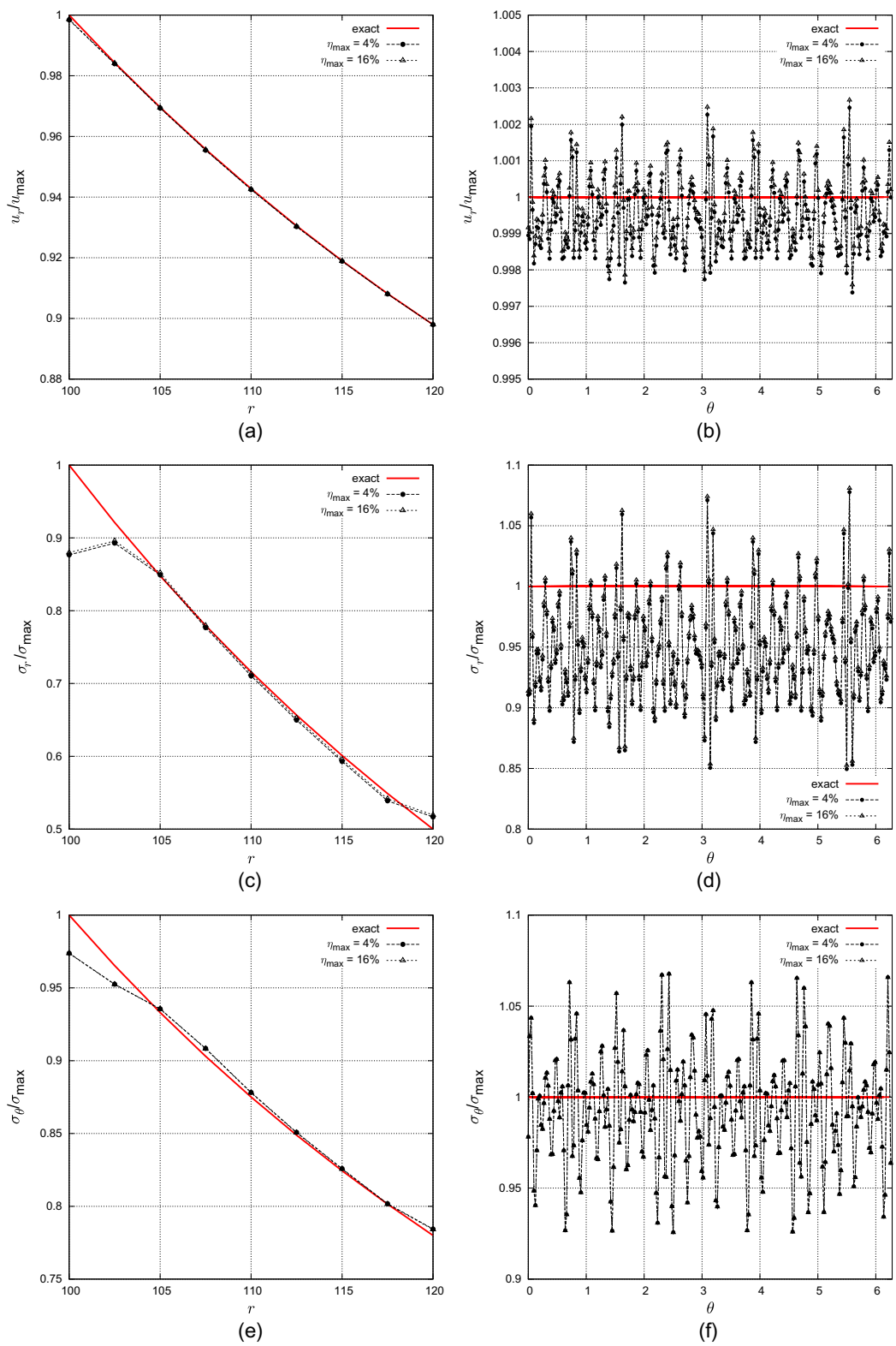

Fig. 5. *Thin* hollow cylinder under pressure: numerical results of the Cauchy problem compared with the analytical solution (u_r, σ_r and σ_θ along the radius, (a), (c) and (e), and on the internal circumference (b), (d) and (f)) noising the pressure on the external circumference with $\eta_{max} = 4\%$ and $\eta_{max} = 16\%$.

$$\mathbf{K}_{uu}\mathbf{w}_u + \mathbf{K}_{ud}\mathbf{w}_d - \mathbf{p}_u = -\mathbf{K}_{uo}\mathbf{w}_o, \tag{2.9}$$
$$\mathbf{K}_{du}\mathbf{w}_u + \mathbf{K}_{dd}\mathbf{w}_d = \mathbf{p}_d - \mathbf{K}_{do}\mathbf{w}_o, \tag{2.10}$$
$$\mathbf{K}_{ou}\mathbf{w}_u + \mathbf{K}_{od}\mathbf{w}_d = \mathbf{p}_o - \mathbf{K}_{oo}\mathbf{w}_o. \tag{2.11}$$

From (2.10) follows

$$\mathbf{w}_d = \mathbf{K}_{dd}^{-1}(\mathbf{p}_d - \mathbf{K}_{do}\mathbf{w}_o - \mathbf{K}_{du}\mathbf{w}_u) \tag{2.12}$$

and so, by using (2.11), we have the system which gives $\mathbf{w}_u$

$$(\mathbf{K}_{ou} - \mathbf{K}_{od}\mathbf{K}_{dd}^{-1}\mathbf{K}_{du})\mathbf{w}_u = \mathbf{p}_o - \mathbf{K}_{oo}\mathbf{w}_o - \mathbf{K}_{od}\mathbf{K}_{dd}^{-1}(\mathbf{p}_d - \mathbf{K}_{do}\mathbf{w}_o). \tag{2.13}$$

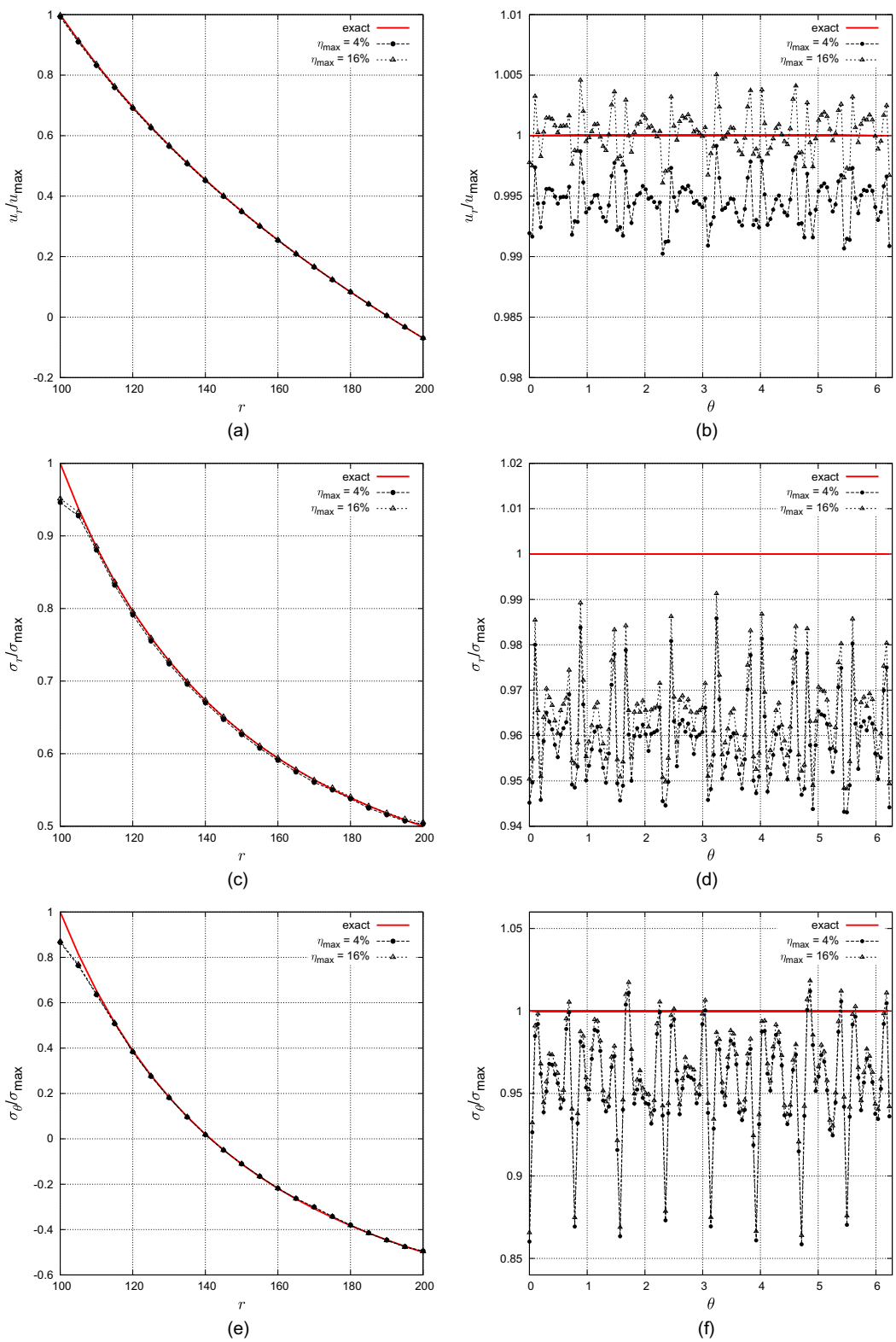

Fig. 6. *Medium* hollow cylinder under pressure: numerical results of the Cauchy problem compared with the analytical solution (u_r, σ_r and σ_θ along the radius, (a), (c) and (e), and on the internal circumference (b), (d) and (f)) noising the pressure on the external circumference with $\eta_{max} = 4\%$ and $\eta_{max} = 16\%$.

Finally, we can easily obtain $\mathbf{w}_d$ by using (2.12) and, successively, $\mathbf{p}_u$ from (2.9):

$$\mathbf{p}_u = \mathbf{K}_{uu}\mathbf{w}_u + \mathbf{K}_{ud}\mathbf{w}_d + \mathbf{K}_{uo}\mathbf{w}_o. \tag{2.14}$$

The core of the three solution steps given by Eqs. (2.12)–(2.14) is the system (2.13) whose main feature is its ill-conditioning. As a result to calculate its solution will be more or less difficult depending on the amount of Cauchy data that can be exploited in the

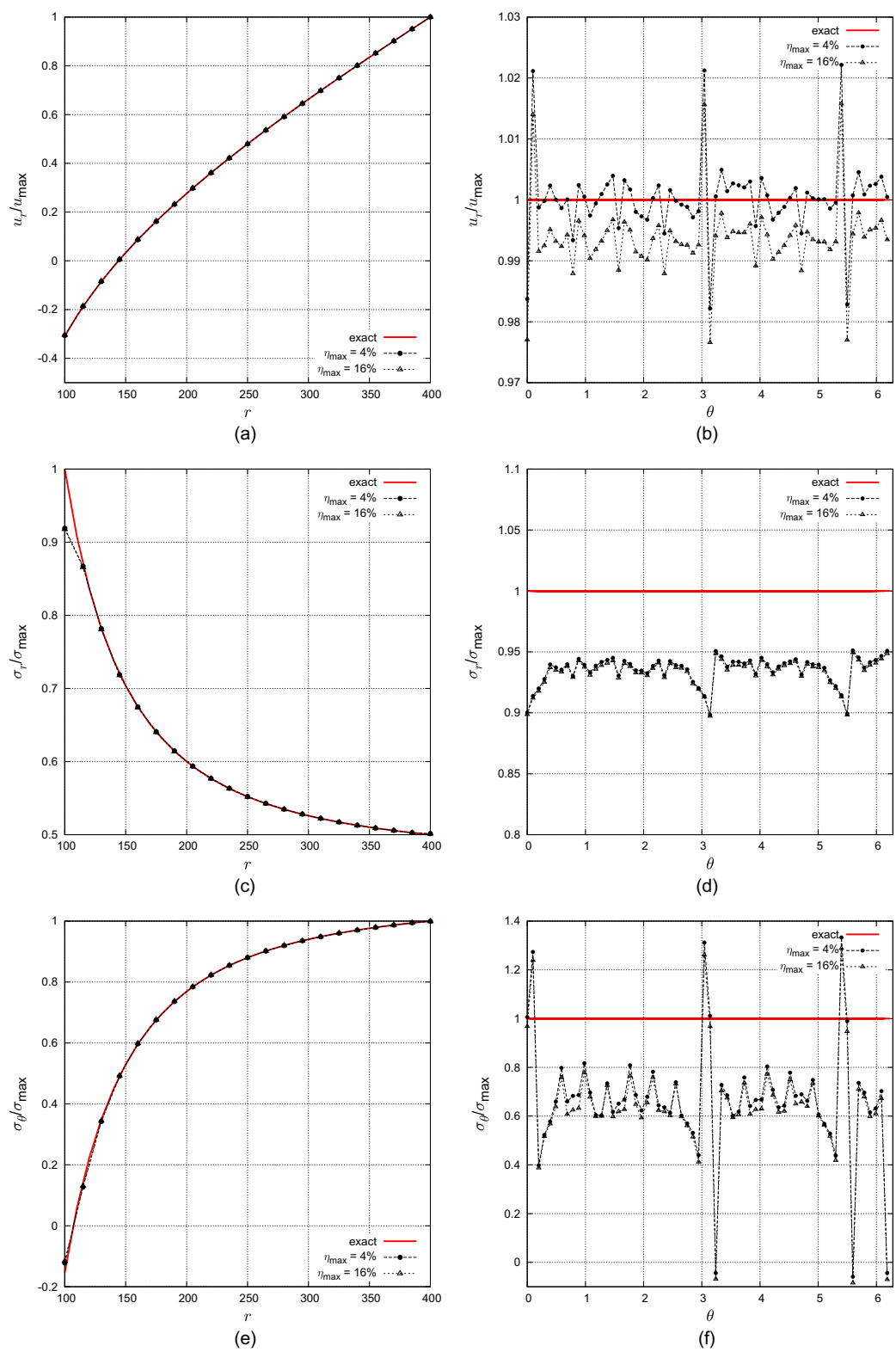

Fig. 7. *Thick* hollow cylinder under pressure: numerical results of the Cauchy problem compared with the analytical solution (u_r, σ_r and σ_θ along the radius, (a), (c) and (e), and on the internal circumference (b), (d) and (f)) noising the pressure on the external circumference with $\eta_{max} = 4\%$ and $\eta_{max} = 16\%$.

solution of this inverse problem, *i.e.* the amount of boundary data relative to the accessible part of the boundary. In particular the system is characterized by a rectangular matrix of dimensions $n_o \times n_u$, where n_o is the number of the overdetermined degrees of freedom and n_u is the number of the underdetermined ones. Obviously, it is more desirable to have a system of equations with more rows than columns, $n_o \geqslant n_u$, especially in the present case of a discrete system of equations derived from a well known ill-posed problem and so very sensitive to the errors certainly contained in the data.

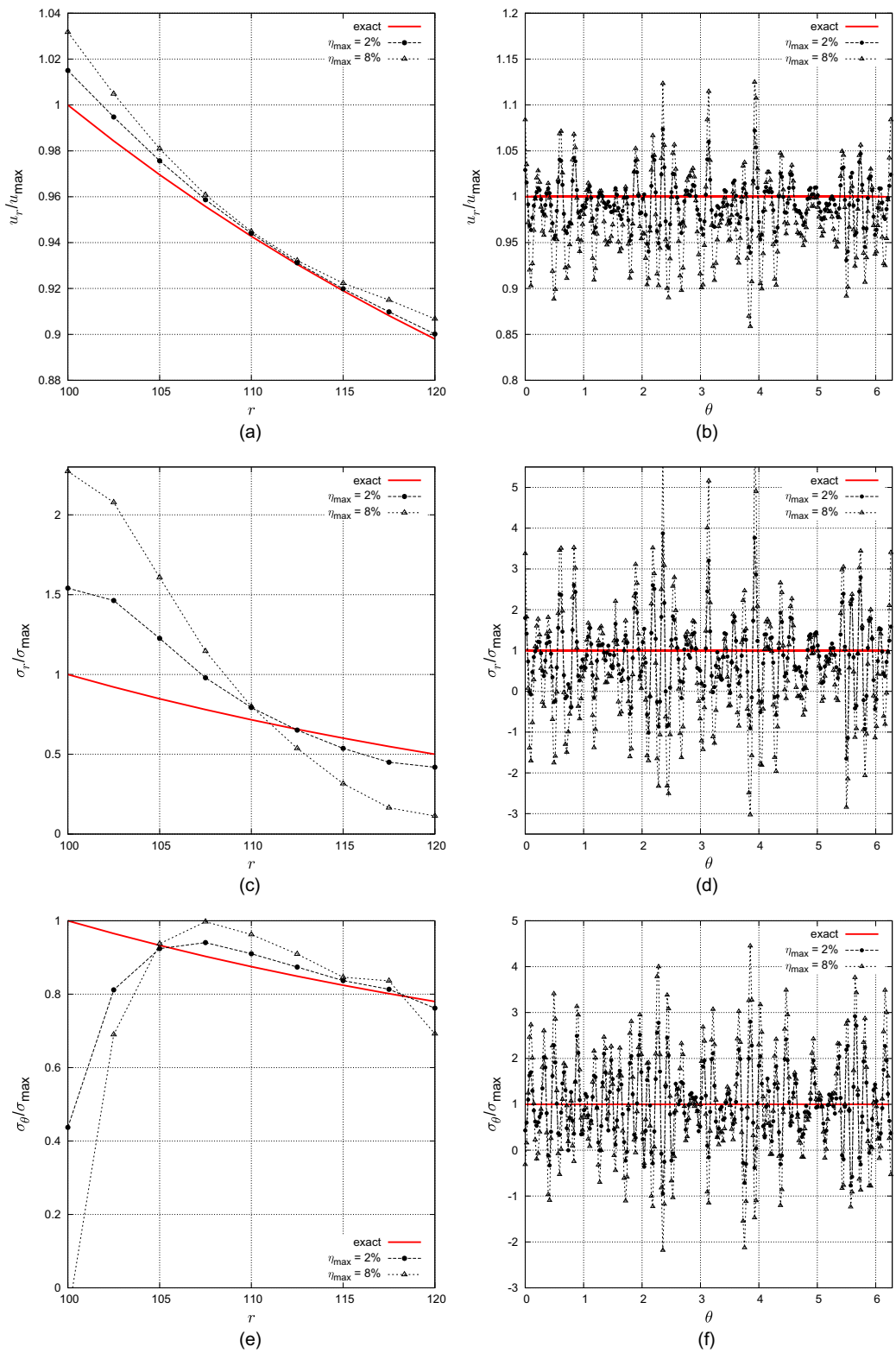

Fig. 8. *Thin* hollow cylinder under pressure: numerical results of the Cauchy problem compared with the analytical solution (u_r, σ_r and σ_θ along the radius, (a), (c) and (e), and on the internal circumference (b), (d) and (f)) noising displacements on the external circumference with $\eta_{max} = 2\%$ and $\eta_{max} = 8\%$.

3. A reconstruction algorithm

The problem to solve is the system given by Eq. (2.13). For the sake of clearness, we will refer to this system of equations using the compact notation

$$\mathbf{A}\mathbf{x} = \mathbf{b}, \tag{3.1}$$

where the matrix $\mathbf{A}$, which has dimension $m \times n$, and the vectors $\mathbf{x}$ and $\mathbf{b}$ of length equal to n and m, respectively, are defined by

$$\mathbf{A} := \mathbf{K}_{ou} - \mathbf{K}_{od}\mathbf{K}_{dd}^{-1}\mathbf{K}_{du}, \ \mathbf{x} := \mathbf{w}_u, \ \mathbf{b} := \mathbf{p}_o - \mathbf{K}_{oo}\mathbf{w}_o - \mathbf{K}_{od}\mathbf{K}_{dd}^{-1}(\mathbf{p}_d - \mathbf{K}_{do}\mathbf{w}_o). \tag{3.2}$$

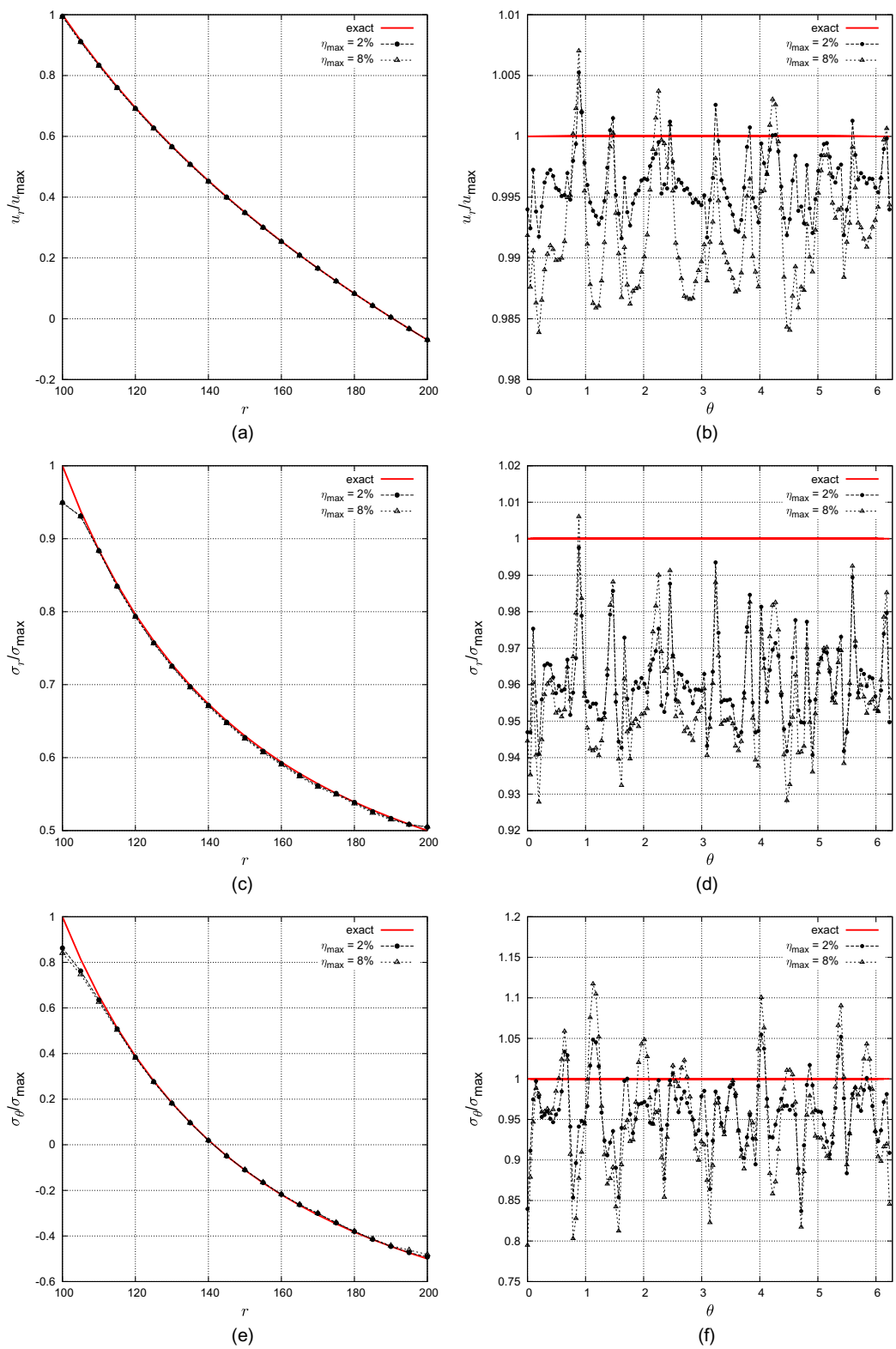

Fig. 9. *Medium* hollow cylinder under pressure: numerical results of the Cauchy problem compared with the analytical solution (u_r, σ_r and σ_θ along the radius, (a), (c) and (e), and on the internal circumference (b), (d) and (f)) noising displacements on the external circumference with $\eta_{max} = 2\%$ and $\eta_{max} = 8\%$.

As already observed, the rectangular linear system of equation (3.1) is ill-conditioned. The main numerical tool available for the analysis of rank-deficient and discrete ill-posed problems is the Singular Value Decomposition of the matrix **A**:

$$\mathbf{A} = \mathbf{U}\boldsymbol{\Sigma}\mathbf{V}^{\mathrm{T}} = \sum_{i=1}^{n} \mathbf{u}_i \sigma_i \mathbf{v}_i^{\mathrm{T}}. \tag{3.3}$$

U and **V**, which have $m \times n$ and $n \times n$ dimensions, respectively, are matrices whose columns are the orthonormal vectors $\mathbf{u}_i$ and $\mathbf{v}_i$, the left and right singular vectors, and $\boldsymbol{\Sigma}$ is a diagonal matrix, with $n \times n$ dimensions, having nonnegative diagonal terms equal to σ_i, the singular values of **A**, see Golub and Van Loan (1996) for details. Such a decomposition makes explicit the degree of ill-conditioning of the

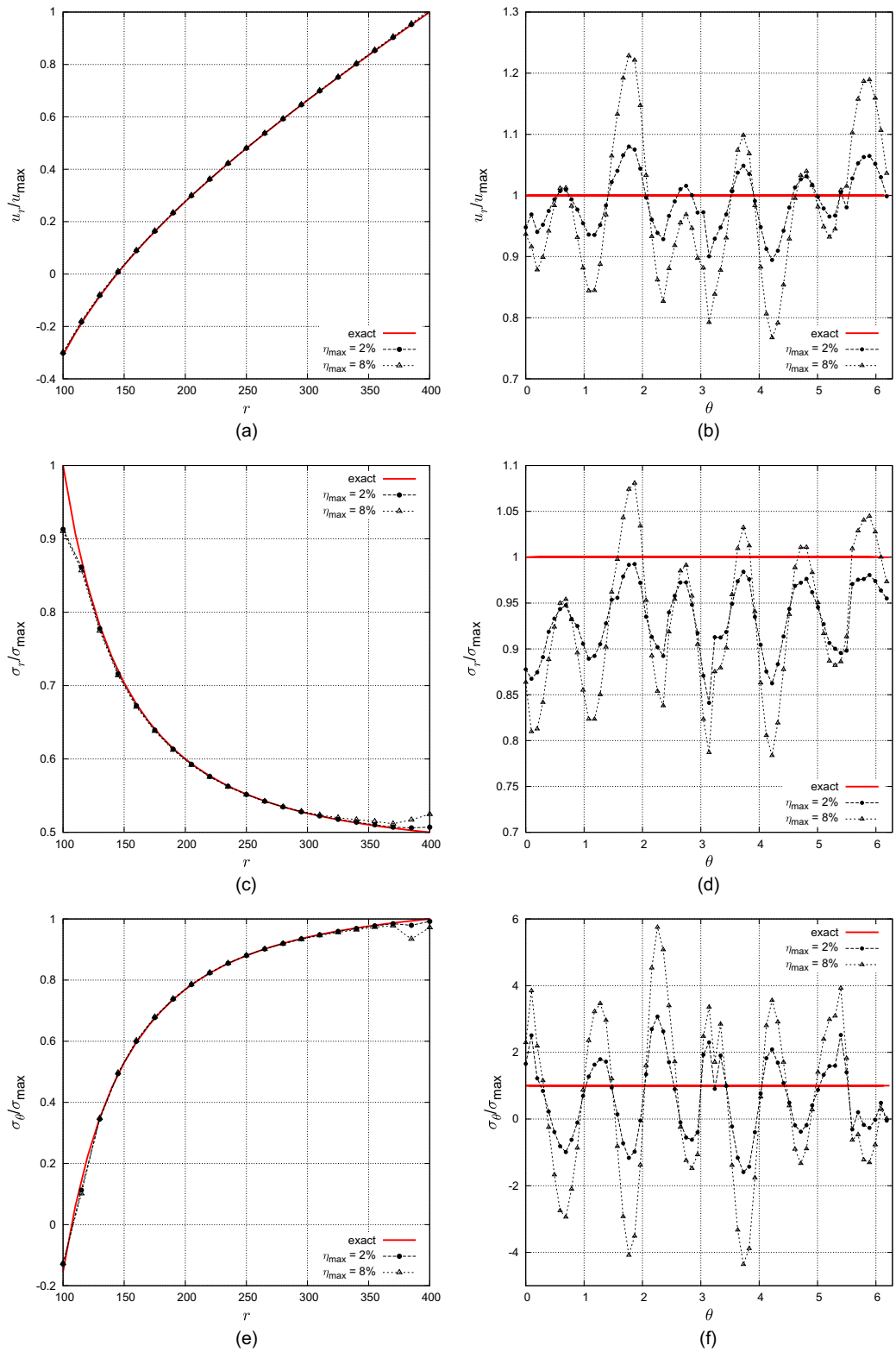

Fig. 10. *Thick* hollow cylinder under pressure: numerical results of the Cauchy problem compared with the analytical solution (u_r, σ_r and σ_θ along the radius, (a), (c) and (e), and on the internal circumference (b), (d) and (f)) noising displacements on the external circumference with $\eta_{max} = 2\%$ and $\eta_{max} = 8\%$.

matrix **A** through the ratio between the maximum and the minimum singular value but also allows to write the solution of the system (3.1) in the following form:

$$\mathbf{x} = \sum_{i=1}^{n} \frac{\mathbf{u}_i^{\mathrm{T}}\mathbf{b}}{\sigma_i}\mathbf{v}_i. \tag{3.4}$$

The latter equation clearly brings out the difficulties connected to the solution of ill-posed discrete problems for which the presence of very small singular values can strongly corrupt the quality of the solution. In addition, it is important to stress that the known term **b** contains errors deriving from modeling, discretization and

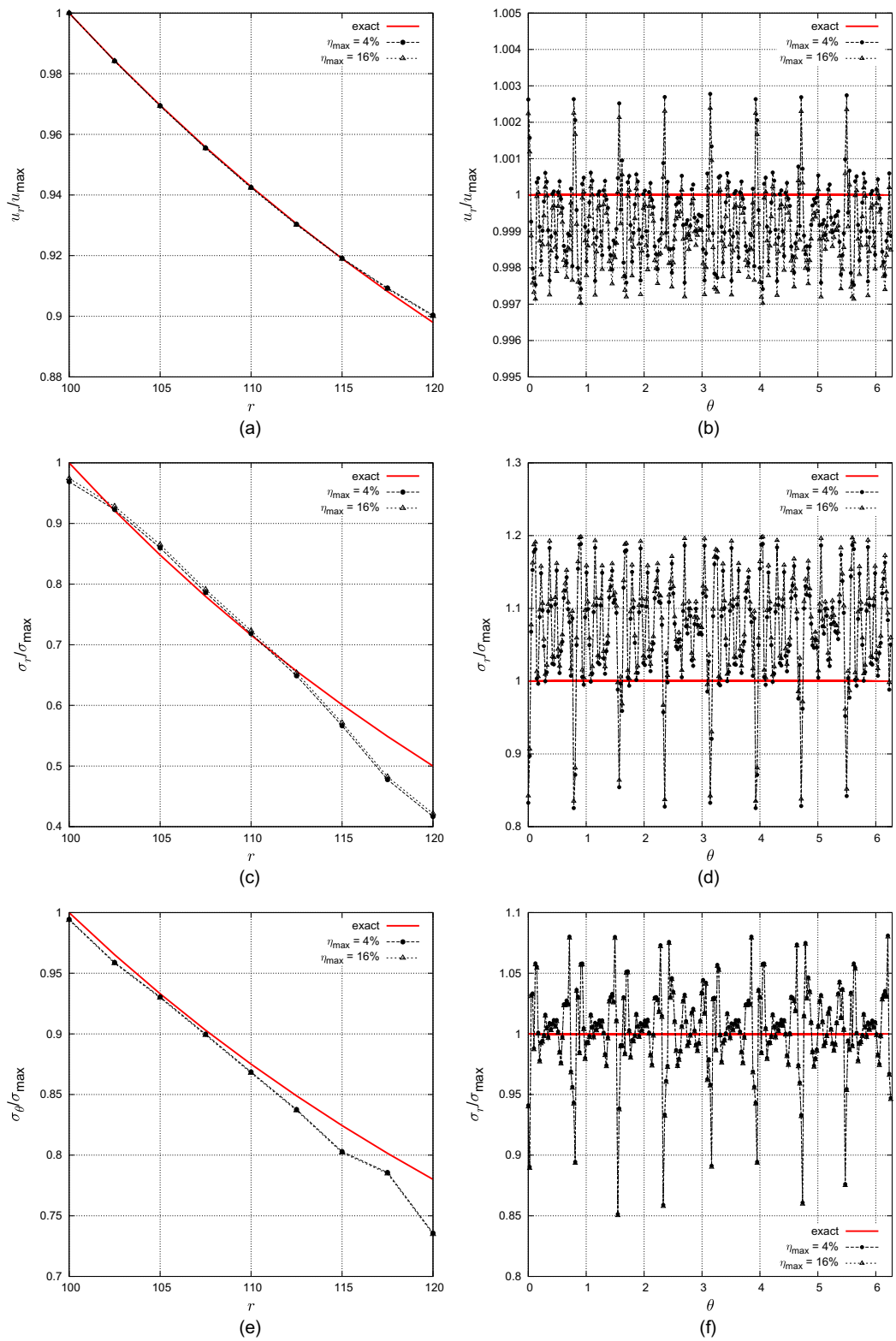

Fig. 11. *Thin* hollow cylinder under pressure: numerical results of the Cauchy problem compared with the analytical solution (u_r, σ_r and σ_θ along the radius, (a), (c) and (e), and on the internal circumference (b), (d) and (f)) noising the pressure on the internal circumference with $\eta_{max} = 4\%$ and $\eta_{max} = 16\%$.

measurements and all these errors are doomed to be amplified in the solution by the contributions related to the smallest singular values.

A way to tackle with the ill-conditioning of the system and to filter out the errors present in the known term is to use the Tikhonov regularization (Tikhonov and Arsenin, 1977). The approach starts from a least square reformulation of (3.1)

$$\min\{\|\mathbf{Ax}-\mathbf{b}\|^2\}, \tag{3.5}$$

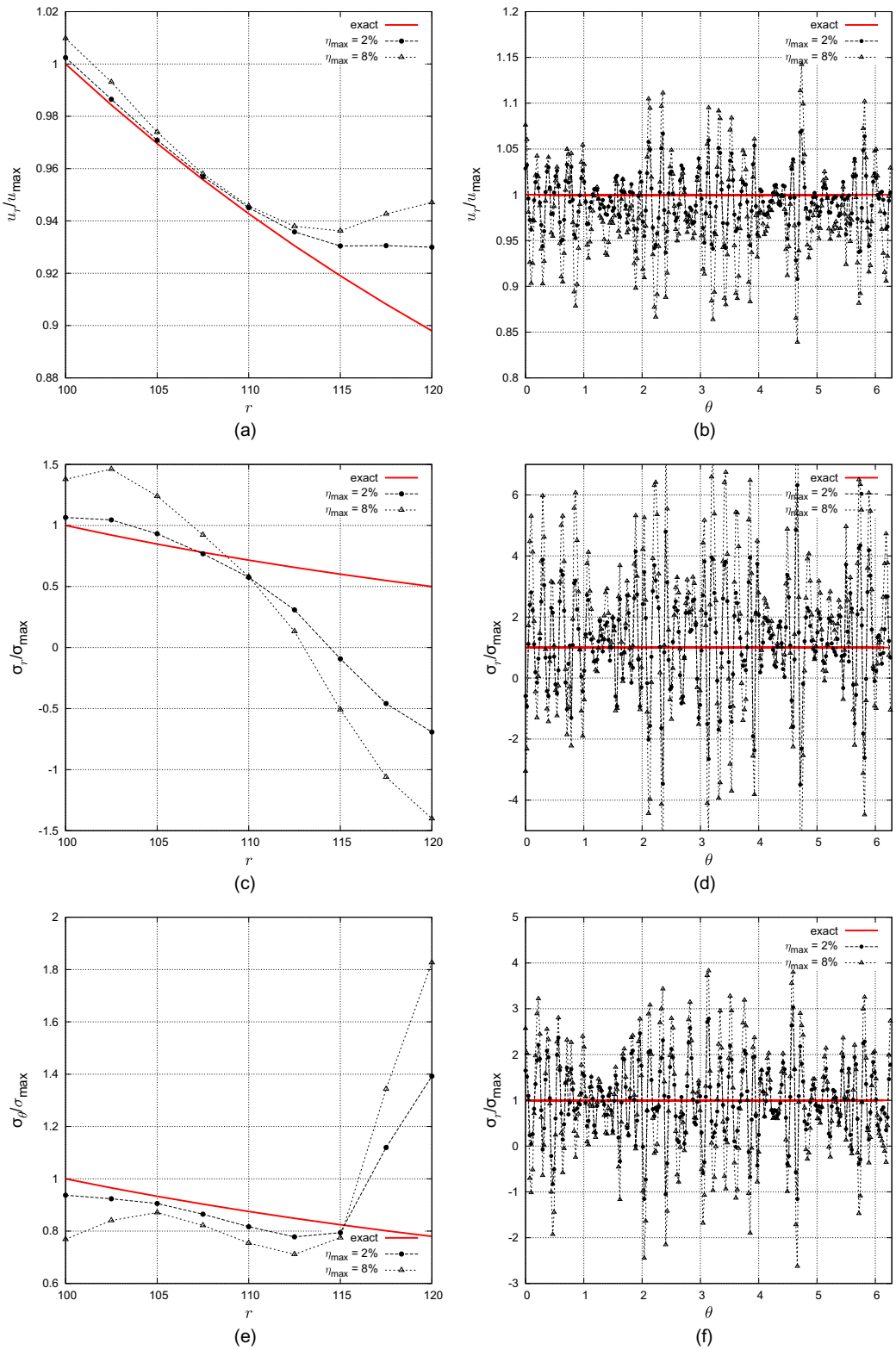

Fig. 12. *Thin* hollow cylinder under pressure: numerical results of the Cauchy problem compared with the analytical solution (u_r, σ_r and σ_θ along the radius, (a), (c) and (e), and on the internal circumference (b), (d) and (f)) noising displacements on the internal circumference with $\eta_{max} = 2\%$ and $\eta_{max} = 8\%$.

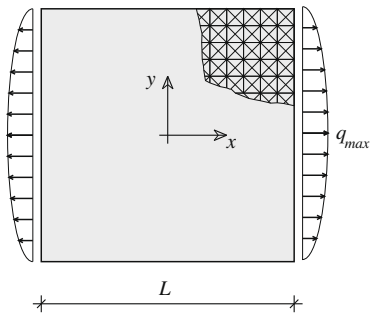

Fig. 13. Square plate stretched by a parabolic load.

and adds a stabilizing term incorporating an *a priori* assumption above the size of the searched solution, *i.e.*

$$\min\left\{\|\mathbf{A}\mathbf{x}-\mathbf{b}\|_P^2+\lambda^2\|\mathbf{x}-\mathbf{x}_0\|_Q^2\right\}, \tag{3.6}$$

where $\mathbf{x}_0$ is an estimate of the solution which can be also the null vector when no information on the solution is available, the weighted norms $\|\mathbf{a}\|_P^2$ and $\|\mathbf{a}\|_Q^2$ are simply defined as $\mathbf{a}^{\mathrm{T}}\mathbf{P}\mathbf{a}$ and $\mathbf{a}^{\mathrm{T}}\mathbf{Q}\mathbf{a}$, respectively, where $\mathbf{P}$ and $\mathbf{Q}$ are two matrices opportunely defined and λ^2, the *regularization parameter*, controls the weight given to minimization of the regularization term. Problem (3.6) can be interpreted in various ways. The most simple is to look at the stabilizing term as a constraint by means of the Lagrange multiplier λ^2. This regularize the problem making it well-posed substantially shifting the singular values of the matrix $\mathbf{A}$ of λ^2. The solution of problem (3.6), in the case $\mathbf{P}=\mathbf{Q}=\mathbf{I}$ and $\mathbf{x}_0=\mathbf{0}$, is given by

$$\mathbf{x}=\sum_{i=1}^{n}\sigma_i\frac{\mathbf{u}_i^{\mathrm{T}}\mathbf{b}}{\sigma_i^2+\lambda^2}\mathbf{v}_i, \tag{3.7}$$

which coincides with (3.4) for a null value of the regularization parameter. At this point the problem to solve becomes to find a suitable value of the regularizing parameter λ^2 which weights opportunely the system of equations to solve and the constraint on the solution.

Then the focus from the ill-conditioning of the system (3.1) is now on a suitable choice of the regularization parameter to be adopted in the solution of problem (3.6). In this regard many criteria have been proposed, see for example Hansen (1992), but one of the most interesting and widely used is the Generalized Cross Validation criterion proposed in Golub et al. (1979). The main advantage of this criterion is that it does not require any information about the size of error contained in the known term of the system of equations nor on its distribution. Furthermore, it is very simple to code, particularly if the singular values of the system matrix are known.

In order to explain how this criterion works let us denote with $\mathbf{x}_j(\lambda)$ the solution of the problem (3.6), for an assigned value of λ, obtained deleting the jth row of matrix $\mathbf{A}$ and jth data observation, *i.e.* the jth component of $\mathbf{b}$. The residual of this regularized solution can be written as:

$$\|\mathbf{A}\mathbf{x}_j(\lambda)-\mathbf{b}\|^2=\|\mathbf{R}_j(\mathbf{A}\mathbf{x}_j(\lambda)-\mathbf{b})\|^2+\left(\mathbf{A}_j^{\mathrm{T}}\mathbf{x}_j(\lambda)-\mathbf{b}_j\right)^2, \tag{3.8}$$

where $\mathbf{R}_j$ is the operator which deletes the jth row of the system of equations and $\mathbf{A}_j$ is the row of matrix $\mathbf{A}$ deleted. The two quantities in the right hand side of Eq. (3.8) can be easily interpreted, respectively, as the residual of the system of equations without the jth row and the residual of the jth row. The Cross Validation criterion states that the optimal value of the regularization parameter λ should not be related to a single observation. So, looking at Eq. (3.8), the translation in formula of Cross Validation criterion gives:

$$\min\left\{C(\lambda):=\sum_{j=1}^{m}g_j\left(\mathbf{A}_j^{\mathrm{T}}\mathbf{x}_j[\lambda]-\mathbf{b}_j\right)^2\right\}, \tag{3.9}$$

where g_j are the weights given at each observation.

Cross Validation criterion can be generalized by using an additional condition: the optimal value of the regularization parameter must be invariant with respect to any rotation of the coordinate system used for the measurements. This hypothesis, rather reasonable, becomes an implicit condition for weights g_j and produces the Generalized Cross Validation criterion:

$$\min\left\{G(\lambda):=\frac{\mathbf{r}_\lambda^{\mathrm{T}}\mathbf{r}_\lambda}{\left(\mathrm{tr}\left(\mathbf{I}-\widehat{\mathbf{A}}\right)\right)^2}\right\}. \tag{3.10}$$

The latter minimization problem gives the optimal value of the regularization parameter λ. In (3.10) $\mathbf{r}_\lambda$ is the residual for an assigned λ, $\mathrm{tr}(\cdot)$ is the trace operator and $\widehat{\mathbf{A}}$ is formally given by:

$$\widehat{\mathbf{A}}=\mathbf{A}\left(\mathbf{A}^{\mathrm{T}}\mathbf{A}+\lambda^2\mathbf{I}\right)^{-1}\mathbf{A}^{\mathrm{T}}. \tag{3.11}$$

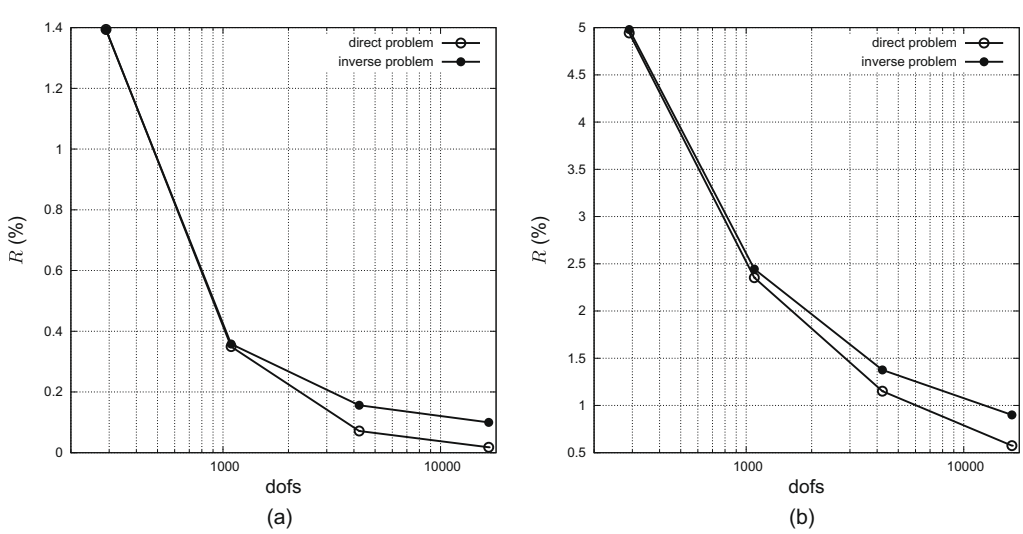

Fig. 14. Square plate stretched by a parabolic load: global error index R *versus* the size, expressed in number of degrees of freedom, of the mesh; error in the displacement field (a) and error in the displacement gradient field (b).

Whereas it is very simple to evaluate the numerator of the Eq. (3.10), the calculation of the denominator appears more difficult. However, if the singular values σ_i of the matrix $\mathbf{A}$ are known, its evaluation is very simple using the expression proposed in Golub et al. (1979):

$$(\mathrm{tr}(\mathbf{I}-\widehat{\mathbf{A}}))^2 = m - n + \sum_{i=1}^{n}\left(\frac{\lambda^2}{\lambda^2+\sigma_i^2}\right). \tag{3.12}$$

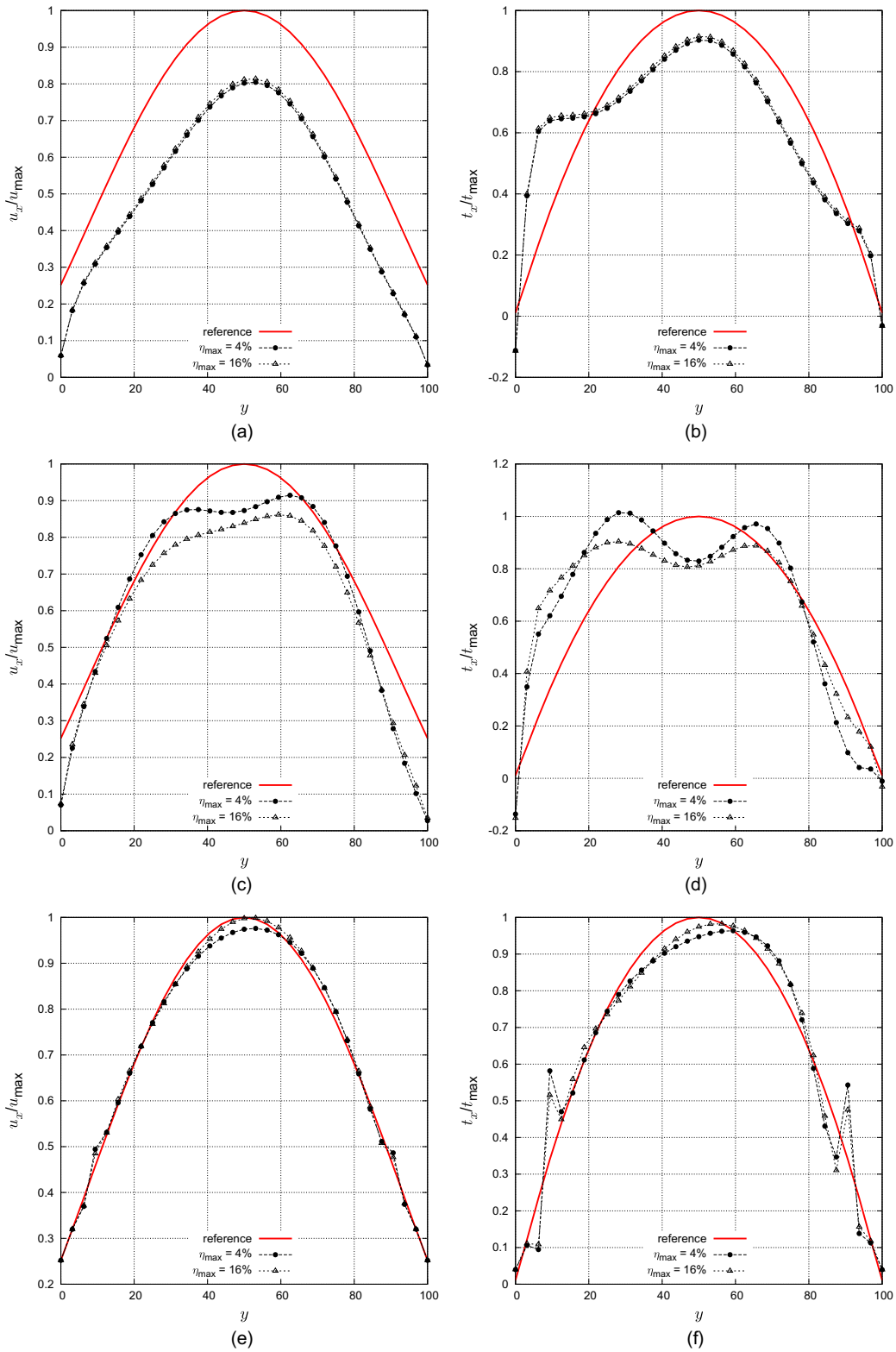

Fig. 15. Square plate stretched by a parabolic load: numerical results of the Cauchy problem compared with the reference solution for u_x (a, c, e) and t_x (b, d, f) on the side $x = -L/2$ for $\ell_o/\ell_u = 1/3$ (a, b), $\ell_o/\ell_u = 1$ (c, d), and $\ell_o/\ell_u = 3$ (e, f) noising tractions by using $\eta_{max} = 4\%,16\%$.

4. Numerical results

The numerical approach described in the previous sections has been implemented in an in-house code based on standard Constant Strain Triangles (CST) elements for setting up the FEM discretization and on the GNU scientific library for calculating the Singular Value Decomposition of the system matrix and minimizing the Generalized Cross Validation objective function. This numerical tool has been used to perform an in-depth numerical study in order to measure the degree of confidence in the analysis of Cauchy

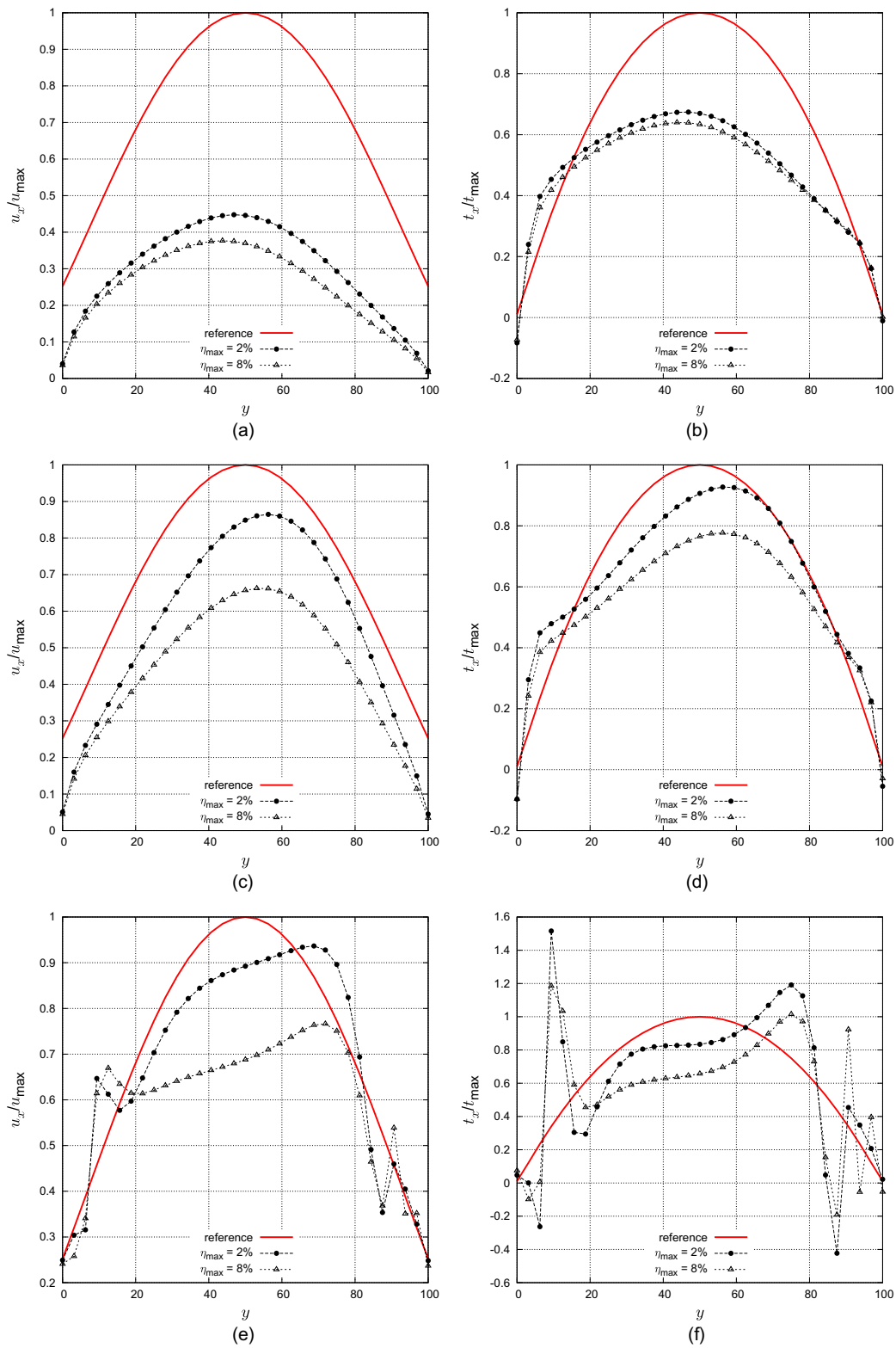

Fig. 16. Square plate stretched by a parabolic load: numerical results of the Cauchy problem compared with the reference solution for u_x (a, c, e) and t_x (b, d, f) on the side $x = -L/2$ for $\ell_o/\ell_u = 1/3$ (a, b), $\ell_o/\ell_u = 1$ (c, d), and $\ell_o/\ell_u = 3$ (e, f) noising displacements by using $\eta_{max} = 2\%.8\%$.

Table 2
Square plate stretched by a parabolic load: boundary data for the Cauchy problem.

ℓ_o/ℓ_u	
1/3	u_x, u_y, t_x, t_y on $\{x = L/2, \lvert y\rvert \leqslant L/2\}$
1	u_x, u_y, t_x, t_y on $\{x = L/2, \lvert y\rvert \leqslant L/2\} \cup \{0 < x \leqslant L/2, y = \pm L/2\}$
3	u_x, u_y, t_x, t_y on $\{x = L/2, \lvert y\rvert \leqslant L/2\} \cup \{\lvert x\rvert \leqslant L/2, y = \pm L/2\}$

problems in two-dimensional elasticity. In particular, we have tried to highlight the sensitivity to the following parameters:

- the amount of Cauchy data available to solve the problem;
- the noise contained in the boundary data;
- the regularization parameter;

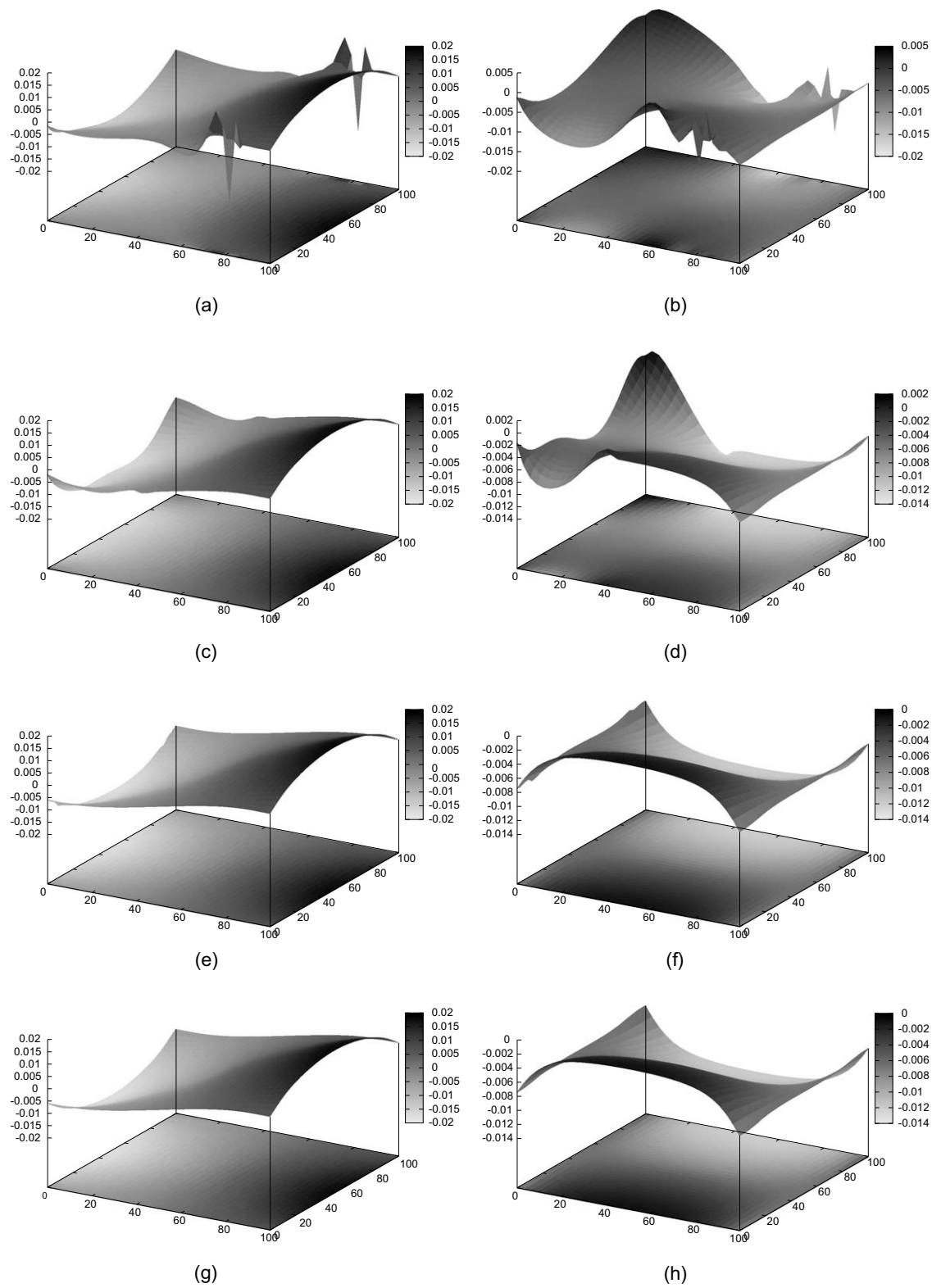

Fig. 17. Square plate stretched by a parabolic load: numerical results of the Cauchy problem for u_x (a, c, e) and u_y (b, d, f) on the domain for $\ell_o/\ell_u = 1/3$ (a, b), $\ell_o/\ell_u = 1$ (c, d), and $\ell_u/\ell_o = 3$ (e, f) noising tractions with $\eta_{\max} = 4\%$ compared with the reference solution (g, h).

- the discontinuity in the boundary conditions to reconstruct;
- the mesh refinement.

The sensitivity to the amount of Cauchy data available to solve the problem has been tested using as parameter the ratio ℓ_o/ℓ_u, where ℓ_o is the length of the overdetermined part of boundary and ℓ_u is the length of the underdetermined part. However, the following numerical results highlight also the influence of which part of the boundary is overdetermined and its position relatively to the underdetermined part. The sensitivity to the noise affecting the

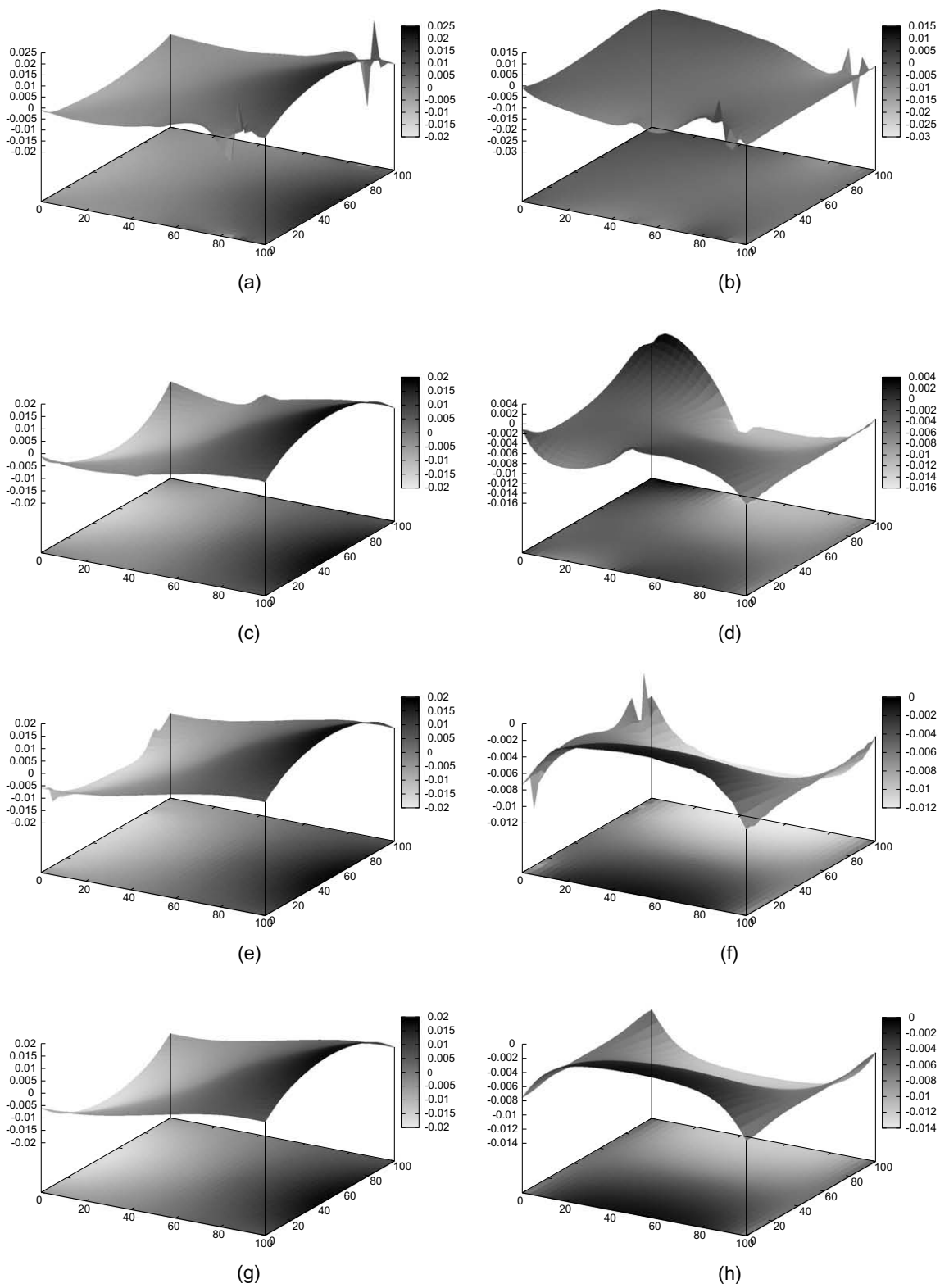

Fig. 18. Square plate stretched by a parabolic load: numerical results of the Cauchy problem for u_x (a, c, e) and u_y (b, d, f) on the domain for $\ell_o/\ell_u = 1/3$ (a, b), $\ell_o/\ell_u = 1$ (c, d), and $\ell_o/\ell_u = 3$ (e, f) noising displacements with $\eta_{\max} = 2\%$ compared with the reference solution (g, h).

known boundary data has been tested by perturbing separately the boundary tractions and the boundary displacements. The influence of the regularization parameter was studied in the frame of the Tikhonov approach using as criterion to select the *optimal* solution the Generalized Cross Validation. The reconstruction of discontinuous boundary conditions was considered by keeping in mind that this is a goal very difficult to achieve in the frame of the regularization approach which naturally tends to select smooth solution. Sensitivity to mesh refinement was studied by comparing the convergence rates given by the FEM discretizations in the analysis of the Cauchy problem and of the corresponding direct problem.

The simulation of the noise affecting the Cauchy data requires some specifications since it strongly influences the solution of all inverse problems. In the solution of an actual problem both imposed and measured boundary conditions derive from instruments and so errors deriving from their inaccuracy are expected. In our study, we are not interested in representing these errors accurately then we have chosen to generate their inaccuracy by perturbing the data used as input for the Cauchy problem. These data are assigned through the analytical solution, if it is known, or by using the best FEM solution obtained by solving the corresponding direct problem. In this case the direct problem is solved on a very refined mesh in order to minimize the discretization error. Then an error η_i is added to the ith Cauchy datum d_i obtaining the *actual* datum which simulate the inaccuracy on it, as for example those deriving from the instrument inaccuracy,

$$\tilde{d}_i = d_i + \eta_i. \tag{4.1}$$

The error η_i is extracted from the normal distribution with mean $\mu = 0$ and standard deviation σ. If $P(\cdot)$ denotes the probability, from the property of the normal distribution, we have

$$P(\mu - 3\sigma \leqslant \eta_i \leqslant \mu + 3\sigma) = 99.7\%. \tag{4.2}$$

This signify that is possible to extract an error which is not greater than $\eta_{\max} = 3\sigma$ with a probability equal to 99.7%. The quantity $\eta_{\max}$, named noise level, was chosen as parameter representa-

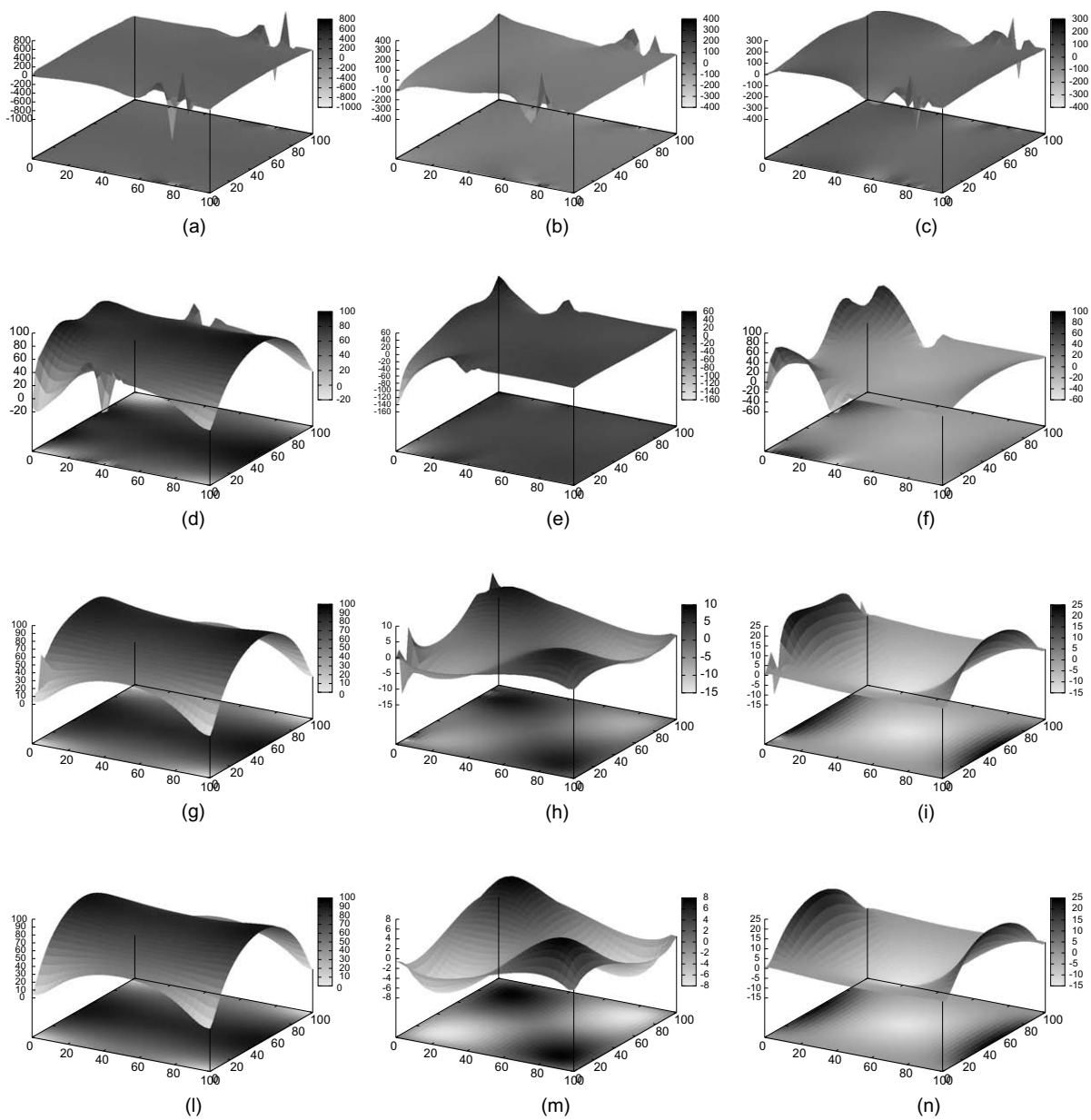

Fig. 19. Square plate stretched by a parabolic load: numerical results of the Cauchy problem for σ_x (a, d, g), σ_{xy} (b, e, h) and σ_y (c, f, i) on the domain for $\ell_o/\ell_u = 1/3$ (a, b, c), $\ell_o/\ell_u = 1$ (d, e, f), and $\ell_o/\ell_u = 3$ (g, h, i) noising tractions with $\eta_{\max} = 4\%$ compared with the reference solution (l, m, n).

tive of the data errors since has an immediate meaning. In general other sources of error could affect the accuracy of the solution, such as errors deriving from the mechanical model used, but they are not considered in the present study.

An additional explanation is required by the method used to apply the assigned noise level to the boundary Cauchy data. In the case of Dirichlet data the noise was applied, independently, to each nodal displacement belonging to the overdetermined boundary. In the case of Neumann data the noise was applied to the intensity of the applied traction, without affecting its shape, and from this perturbed traction all the nodal forces belonging to the overdetermined boundary were recalculated.

The following plane stress problems were studied:

1. a hollow cylinder subjected to uniform pressure on the inner and the outer surfaces;
2. a stretched square plate.

4.1. Hollow cylinder under pressure

The first test proposed is the analysis of a hollow cylinder subjected along the internal and external boundary to a pressure, see Fig. 1. This test was chosen because the analytic solution is known, for the case of plane stress condition the solution is reported in Timoshenko and Goodier (1970), and also because no kind of singularity, in geometry of the domain or boundary conditions, is present. Moreover, this kind of problem can have some interesting practical applications. The analytical solution for the radial displacement $u_r(r)$, the radial stress $\sigma_r(r)$ and the circumferential stress $\sigma_\theta(r)$ is given by

$$u_r(r) = \frac{1}{E}\left(-\frac{1+\nu}{Ar} + (1-\nu)Cr\right), \tag{4.3}$$

$$\sigma_r(r) = \frac{A}{r^2} + C, \tag{4.4}$$

$$\sigma_\theta(r) = -\frac{A}{r^2} + C, \tag{4.5}$$

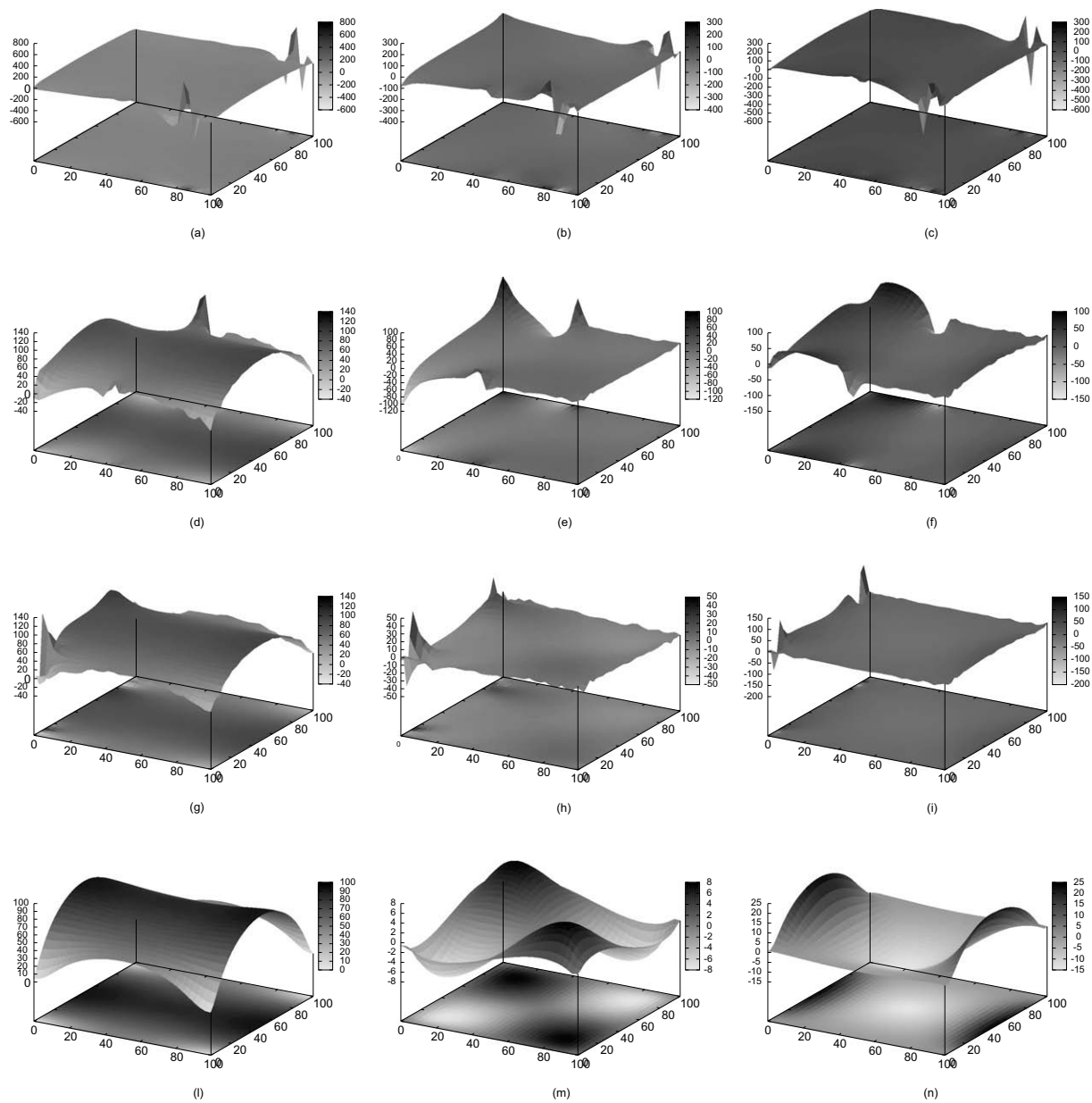

Fig. 20. Square plate stretched by a parabolic load: numerical results of the Cauchy problem for σ_x (a, d, g), σ_{xy} (b, e, h) and σ_y (c, f, i) on the domain for $\ell_o/\ell_u = 1/3$ (a, b, c), $\ell_o/\ell_u = 1$ (d, e, f), and $\ell_o/\ell_u = 3$ (g, h, i) noising displacements with $\eta_{\max} = 2\%$ compared with the reference solution (l, m, n).

where r indicates the distance from the center of the hollow cylinder, E and ν are the Young modulus and the Poisson ratio, respectively, while the coefficients A and C, expressed by using the internal, R_i, and the external, R_e, radius and the internal, p_i, and the external, p_e, pressure, see again Fig. 1, are

$$A = \frac{R_i^2 R_e^2 (p_e - p_i)}{R_e^2 - R_i^2}, \tag{4.6}$$

$$C = \frac{p_i R_i^2 - p_e R_e^2}{R_e^2 - R_i^2}. \tag{4.7}$$

Three types of geometries have been considered: a *thin* hollow cylinder with $R_i = 100$ mm and $R_e = 120$ mm, a *medium* hollow cylinder with $R_i = 100$ mm and $R_e = 200$ mm and a *thick* hollow cylinder with $R_i = 100$ mm and $R_e = 400$ mm. These different geometries allow to test the sensitivity to the distance between the boundary data to reconstruct, those on the inner boundary, from the known data relative to the outer boundary. The values for the internal and external pressure are $p_i = 100$ MPa and $p_e = 50$ MPa, respectively, the Young modulus is $E = 200,000$ MPa and the Poisson ratio is $\nu = 0.29$.

In order to select a suitable mesh for the inverse analysis, *i.e.* a mesh characterized by an acceptable trade-off between accuracy and computational costs, the meshes reported in Table 1 have been used to perform a direct analysis. For each mesh the three numbers reported in Table 1 indicate the number of elements which are imposed in the mesh generation along the interior boundary, the exterior boundary and the radius, respectively. For example, Fig. 1 reports the geometry of the *thick* hollow cylinder and the mesh $32 \times 64 \times 10$.

Figs. 2–4 compare the analytical solution, reported in Timoshenko and Goodier (1970), with the numerical results obtained by solving the direct problem. In particular the comparison regards the radial displacement u_r, the radial stress σ_r and the circumferential stress σ_θ evaluated along the radius for the three cases analyzed, *thin*, *medium* and *thick*, respectively. The plotted values are normalized with respect to the maximum value given by the exact solution in the observed range. From Figs. 2–4, in particular part (b), only the finer mesh, $256 \times 256 \times 8$ for the *thin* and $128 \times 192 \times 20$ for the *medium* hollow cylinder, allow to obtain an enough accurate solution while the mesh $64 \times 128 \times 20$ is acceptable for the *thick* hollow cylinder. Consequently, these meshes have been used to perform the analyses of the Cauchy problems.

In the following tests the Cauchy problem has been solved assuming the exterior circumference as the overdetermined

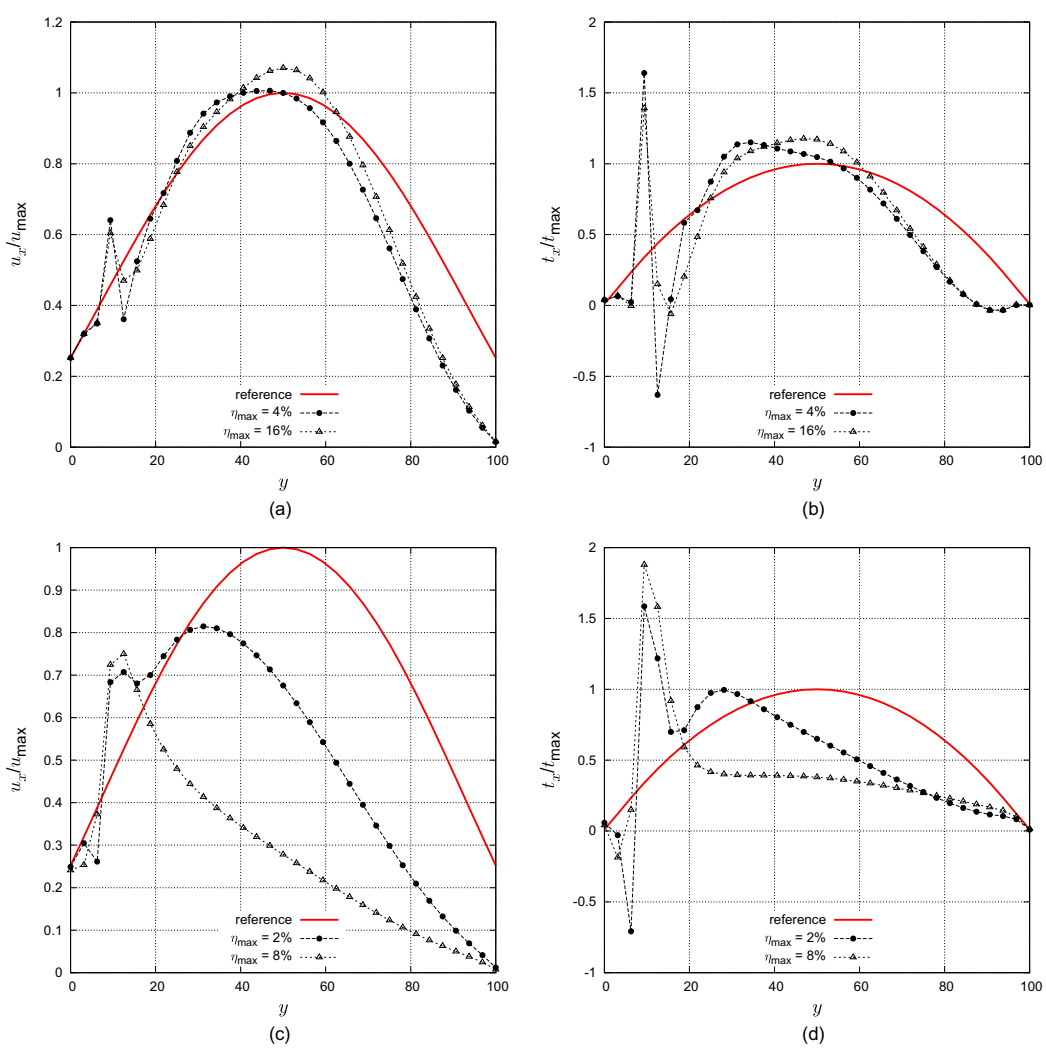

Fig. 21. Square plate stretched by a parabolic load: numerical results of the Cauchy problem for u_x (a, c) and t_x (b, d) on the side $x = -L/2$ noising tractions with $\eta_{max} = 4\%,16\%$ (a, b) and displacements with $\eta_{max} = 2\%,8\%$ (c, d) in the case $\ell_o/\ell_u = 1$ (sides $x = -L/2$ and $y = -L/2$ underdetermined, sides $x = L/2$ and $y = L/2$ overdetermined) compared with the reference solution.

boundary and the interior circumference as the underdetermined one. In this way the ratio ℓ_o/ℓ_u is equal to 1.2 in the case of the *thin* hollow cylinder, 2 in the *medium* case and 4 in the *thick* case. On the overdetermined boundary the known data, displacements and pressure, are assigned on the basis of the analytical solution which is noised in three different ways. In a case the noising is applied only to the value of the external pressure on the basis of the procedure explained in the previous section. In another case the noising is applied, following the same procedure, only to the values of the nodal displacements and, finally, applying the noise to both pressure and displacements.

Figs. 5–7 report the solution obtained by solving the Cauchy problem for the *thin*, *medium* and *thick* hollow cylinder, respectively, by perturbing only the pressure. Here the radial displacement u_r, (a, b), the radial stress σ_r, (c, d), and the circumferential stress σ_θ, (e, f) both along the radial direction (a, c, e) and on the inner circumference (b, d, f) are reported. As above all the quantities are normalized with respect to the maximum exact value.

The results reported in Figs. 8–10 are similar to that reported in Figs. 5–7, except for the noising which is applied only to the displacements of the overdetermined part of the boundary.

Finally, as last test, the *thin* hollow cylinder has been analyzed by considering the exterior circumference as the underdetermined boundary and the interior circumference as the overdetermined boundary. The results obtained, see Figs. 11 and 12, show that the main effect of exchanging the roles played by the interior and the exterior boundaries is that the error is now concentrated along the external boundary, for comparison see Figs. 5 and 8.

From the results obtained it is manifest how noising the displacement field has an effect much stronger than noising the pressure. Comparing the graphics relative to the reconstructed solution on the inner boundary, part (b), (d) and (f) of the Figures, wider oscillations of the computed solution can be observed. Also the solution inside the domain, part (a), (c) and (e) of the Figures, highlights a similar pattern with a worsening in the case of the noising applied to displacements. This is true, also if in a different measure, for all the three geometries considered. This kind of behaviour can be imputed mainly to the way used to apply the assigned noise level in the cases of displacement or pressure perturbation. Noising the applied pressure has a smoother effect because implies only a simple rescaling of the nodal forces of the discrete problem. The results relative to the noising of both boundary data, traction and displacements, were not reported because are very similar to the results obtained in the case of the noising applied only to displacements.

Another recognizable trend is the better accuracy noticeable in the figures relative to the *thick* hollow cylinder with respect to figures relative to the *medium* and *thin* case. A result imputable

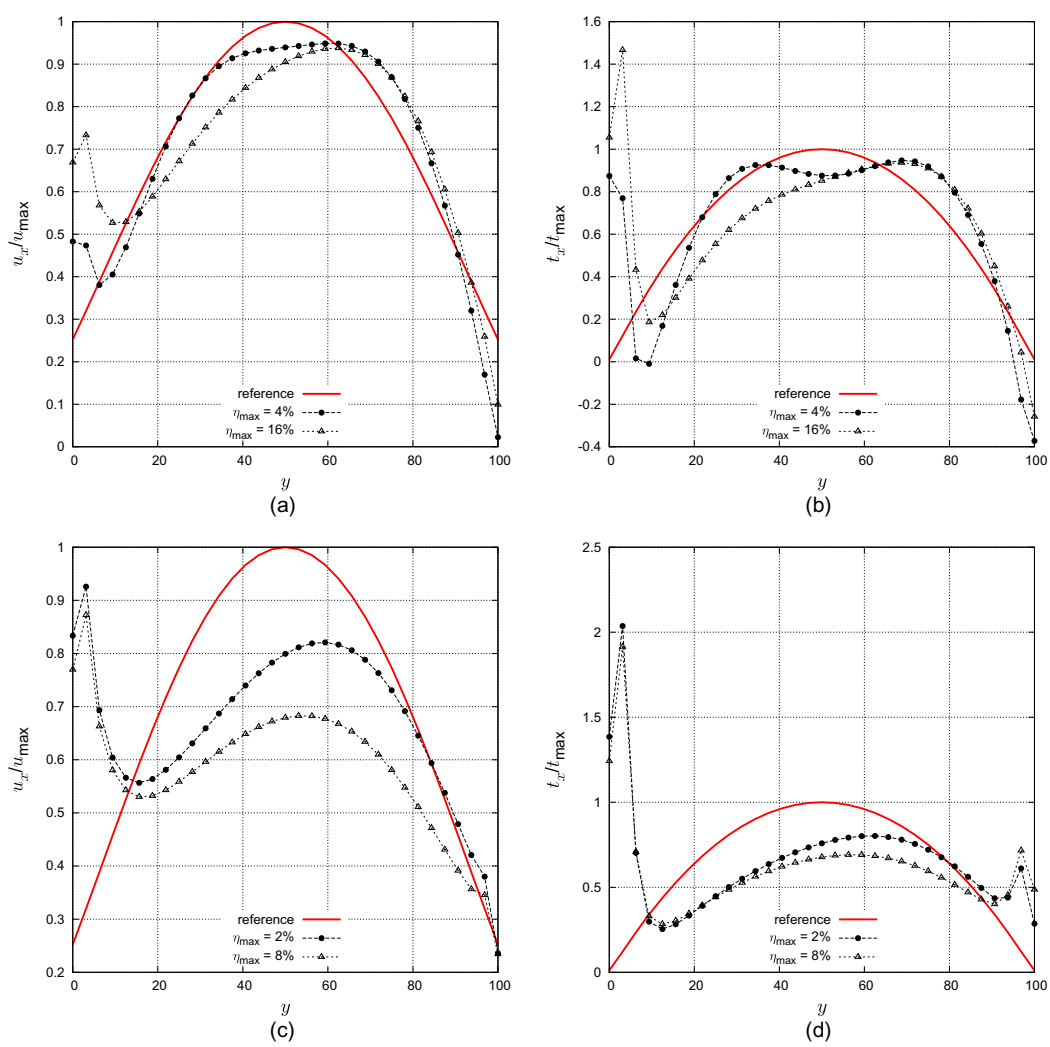

Fig. 22. Square plate stretched by a parabolic load: numerical results of the Cauchy problem for u_x (a, c) and t_x (b, d) on the side $x = -L/2$ noising tractions with $\eta_{max} = 4\%,16\%$ (a, b) and displacements with $\eta_{max} = 2\%,8\%$ (c, d) for $\ell_o/\ell_u = 1, \ell_d/4L = 2$ compared with the reference solution.

mainly to the greater distance of the underdetermined boundary from the overdetermined in the case of the thicker geometry. However, both in the *medium* and in the *thick* case, also the amount of the Cauchy data available for the solution of the inverse problem is greater being $\ell_o/\ell_u = 2$ and $\ell_o/\ell_u = 4$, respectively.

4.2. Stretched square plate

The square plate shown in Fig. 13 was analyzed under plane stress condition. The plate is stretched by a parabolic load with $q_{\max} = 100$ MPa, the length of side L is 100 mm and the chosen con-

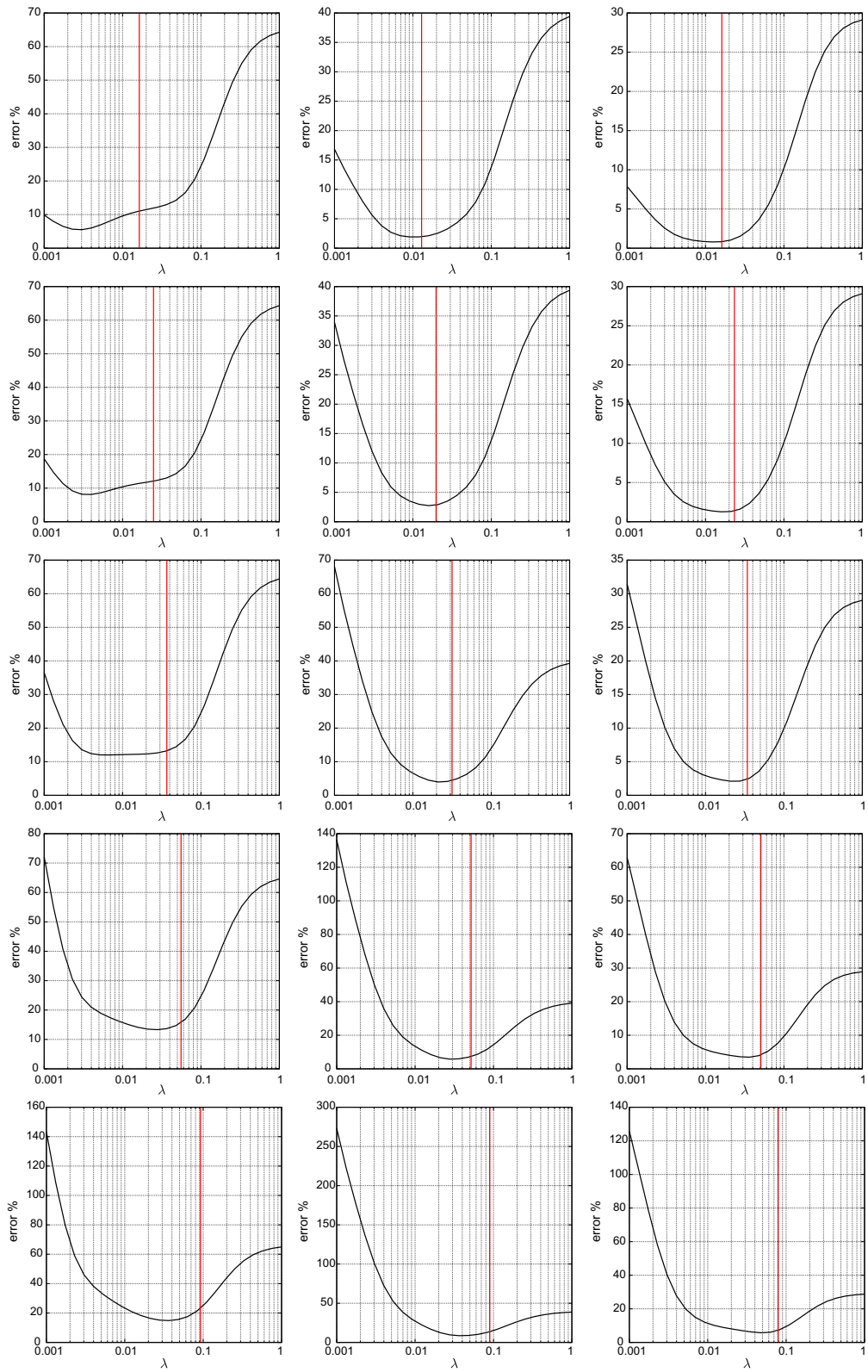

Fig. 23. Stretched square plate: reconstruction error (global error index R relative to the calculated displacement field) *versus* the regularization parameter for $\ell_o/\ell_u = 1/3, 1, 3$ from left to right, and of the data noise level, $\eta_{\max} = 1\%, 2\%, 4\%, 8\%, 16\%$, from top to bottom. In red the value of λ given by the GCV criterion.

stitutive parameter are the Young modulus $E = 200,000$ MPa and the Poisson ratio $\nu = 0.29$. The domain was discretized by using a regular finite element mesh of constant strain triangles. The meshes used are $8 \times 8, 16 \times 16, 32 \times 32, 64 \times 64$ and 128×128, where the numbers indicate the number of squares, each consisting of four triangles, in the two directions, see again Fig. 13. The results obtained from the finest mesh, that is the 128×128 mesh, were used as reference solution.

In the first test the sensitivity to mesh refinement was studied. Fig. 14 reports the displacement and gradient error index R *versus* the number of degrees of freedom of the mesh used ($8 \times 8, 16 \times 16, 32 \times 32$ and 64×64). The error index R is defined as

$$R = \frac{\|z_r - z_{ref}\|_{L_2(\mathscr{B})}}{\|z_{ref}\|_{L_2(\mathscr{B})}}, \tag{4.8}$$

where z_r and z_{ref} are the displacement or the displacement gradient for the obtained numerical solution and the reference solution, respectively, and $\|\cdot\|_{L_2(\mathscr{B})}$ is the L_2-norm over $\mathscr{B}$, see Braess (1997), defined by

$$\|z\|_{L_2(\mathscr{B})} = \left(\int_{\mathscr{B}} z \cdot z \, dA\right)^{1/2}. \tag{4.9}$$

The results were obtained by solving the Cauchy problem assuming as undetermined the part of the boundary with $x < 0$ (all the boundary data are unknown) and as overdetermined its complementary part (all the boundary data is known), then with a ratio $\ell_o/\ell_u = 1$. Furthermore, the prescribed data were applied with zero noise allowing to use a fixed small value of the regularization parameter.

Fig. 14 compares the results obtained in the solution of the inverse problem with that given by the corresponding direct problem. This figure suggests that also with the ratio $\ell_o/\ell_u = 1$, number of data equal to number of unknown, but with no noise in the data, the ill-conditioning of the problem can be easily circumvented through the Tikhonov regularization. The solutions given by the Cauchy and the direct problem are almost coincident for the 8×8 and 16×16 meshes with a little difference for the other meshes which, with the growing of the problem size, trigger the intrinsic instability of the problem. The mesh chosen to perform the inverse analyses is the 32×32 mesh which allows to obtain an acceptable level of accuracy as it is also confirmed by the next numerical tests where the calculated displacement and stress field given by the solution of the Cauchy problem over the 32×32 mesh are compared with that obtained in the solution of the direct problem with the 128×128 mesh. It is noteworthy to observe that the data used to prescribe the Cauchy data for the solution of the inverse problem are taken for the 128×128 mesh, restraining in this way the so-called inverse crime described in Kaipio and Somersalo (2004).

Figs. 15 and 16 report the reconstructed boundary conditions u_x, (a, c, e), and t_x, (b, d, f), along with the reference solution in the case of noise affecting only the known tractions ($\eta_{max} = 4\%,16\%$), Fig. 15, and only the known displacements ($\eta_{max} = 2\%,8\%$), Fig. 16. The tests were performed by changing also the ratio ℓ_o/ℓ_u as reported in Table 2. More precisely (a, b) of Figs. 15 and 16 correspond to $\ell_o/\ell_u = 1/3$, (c, d) to $\ell_o/\ell_u = 1$ and (e, f) to $\ell_o/\ell_u = 3$.

The figures show a significative improvement in the reconstruction of unknown boundary data for higher values of the ratio ℓ_o/ℓ_u, *i.e.* when a greater part of the boundary is accessible. Furthermore, as in the case of the hollow cylinder, noising displacements, see Fig. 16, produces a remarkable deterioration of the reconstructed boundary conditions. The case in which the traction and the displacements are noised was not reported because the tests are dominated by the effect of noising displacements, the obtained results are very similar to that already reported in Fig. 16.

In order to show the quality of the calculated solution also inside the domain, Fig. 17, in the case of noised traction ($\eta_{max} = 4\%$), and Fig. 18, in the case of noised displacements ($\eta_{max} = 2\%$), show the displacement field reconstructed from the solution of the Cauchy problem for the three values of the ratio ℓ_o/ℓ_u considered: parts (a, b) $\ell_o/\ell_u = 1/3$, parts (c, d) $\ell_o/\ell_u = 1$ and parts (e, f) $\ell_o/\ell_u = 3$. The obtained fields are compared with the reference solution, parts (g, h). In the similar way Fig. 19, for noised tractions ($\eta_{max} = 4\%$), and Fig. 20, for noised displacements ($\eta_{max} = 2\%$), show the stress field reconstructed from the solution of the Cauchy problem for the three values of the ratio ℓ_o/ℓ_u considered: parts (a, b, c) $\ell_o/\ell_u = 1/3$, parts (d, e, f) $\ell_o/\ell_u = 1$ and parts (g, h, i) $\ell_o/\ell_u = 3$. For comparison the reference solution is reported in parts (l, m, n). Also these figures, from Figs. 17–20, confirm that the best results are obtained when the amount of known information is greater and when the noising is applied only to the known tractions. However the stress fields obtained in the case of noised displacements, σ_y and σ_{xy} components of Fig. 20, look very flat mainly for the presence of local peaks.

The next test shows the dependence of the reconstructed boundary solution on how the overdetermined boundary is chosen. Fig. 21 reports the results obtained along the side $x = -L/2$ assuming as overdetermined the sides $x = L/2$ and $y = L/2$ and as underdetermined the other sides. In this case $\ell_o/\ell_u = 1$ then the part (a, b) of Fig. 21 has to be compared with the part (c, d) of Fig. 15 and the part (c, d) of Fig. 21 with part (c, d) of Fig. 16. The comparison highlights that in the current case the quality of the solution is poorer. This can be explained by observing that in the current case the Cauchy data available for the solution of the inverse problem are not located following the symmetry of the analyzed problem.

As further test the case in which the boundary is not exactly divided into two parts, one overdetermined and one underdetermined, was considered. In particular the side $x = -L/2$ is underdetermined, the side $x = L/2$ is overdetermined and the sides $y = \pm L/2$ are determined with $t_x = 0$ and $t_y = 0$. Fig. 22 reports, as usual, the reconstruction of u_x (a, c) and t_x (b, d) on the side $x = -L/2$ noising the known traction with $\eta_{max} = 4\%,16\%$ (a, b) and the known displacements with $\eta_{max} = 2\%,8\%$ (c, d). In this case the ratio $\ell_o/\ell_u = 1$ and the reconstructed boundary conditions can be compared with part (c, d) of Fig. 15, noise applied to the known traction, and Fig. 16, noise applied to the known displacements. The quality of the reconstructed displacement and traction field is similar except for a jump on the beginning of the underdetermined side.

Fig. 23 was assembled in order to study how the reconstruction error varies with respect to the regularization parameter λ, considering different values of the ratio ℓ_o/ℓ_u and of the noise level η_{max} in the data. All the plots, reporting the values of the error index al-

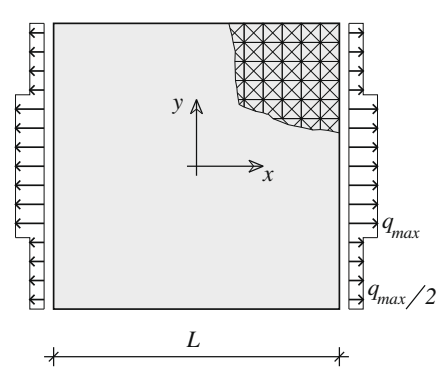

Fig. 24. Square plate stretched with a discontinuous load.

ready defined in (4.8) *versus* the regularization parameter, show, in red, the optimal value selected by the Generalized Cross Validation criterion. We observe that this criterion is robust except for small values of the noise level $\eta_{\max}$ and for the case $\ell_o/\ell_u = 1$ where the criterion tends to overestimate the regularization parameter. Moreover, we observe that the error curve is almost flat in the neighborhood of the optimal value of λ selected by the Generalized Cross Validation criterion and this is an index of stability for the used criterion.

Finally, in order to experiment the difficulties in the reconstruction of discontinuities we have modified the applied load by considering that reported in Fig. 24. Exact and reconstructed

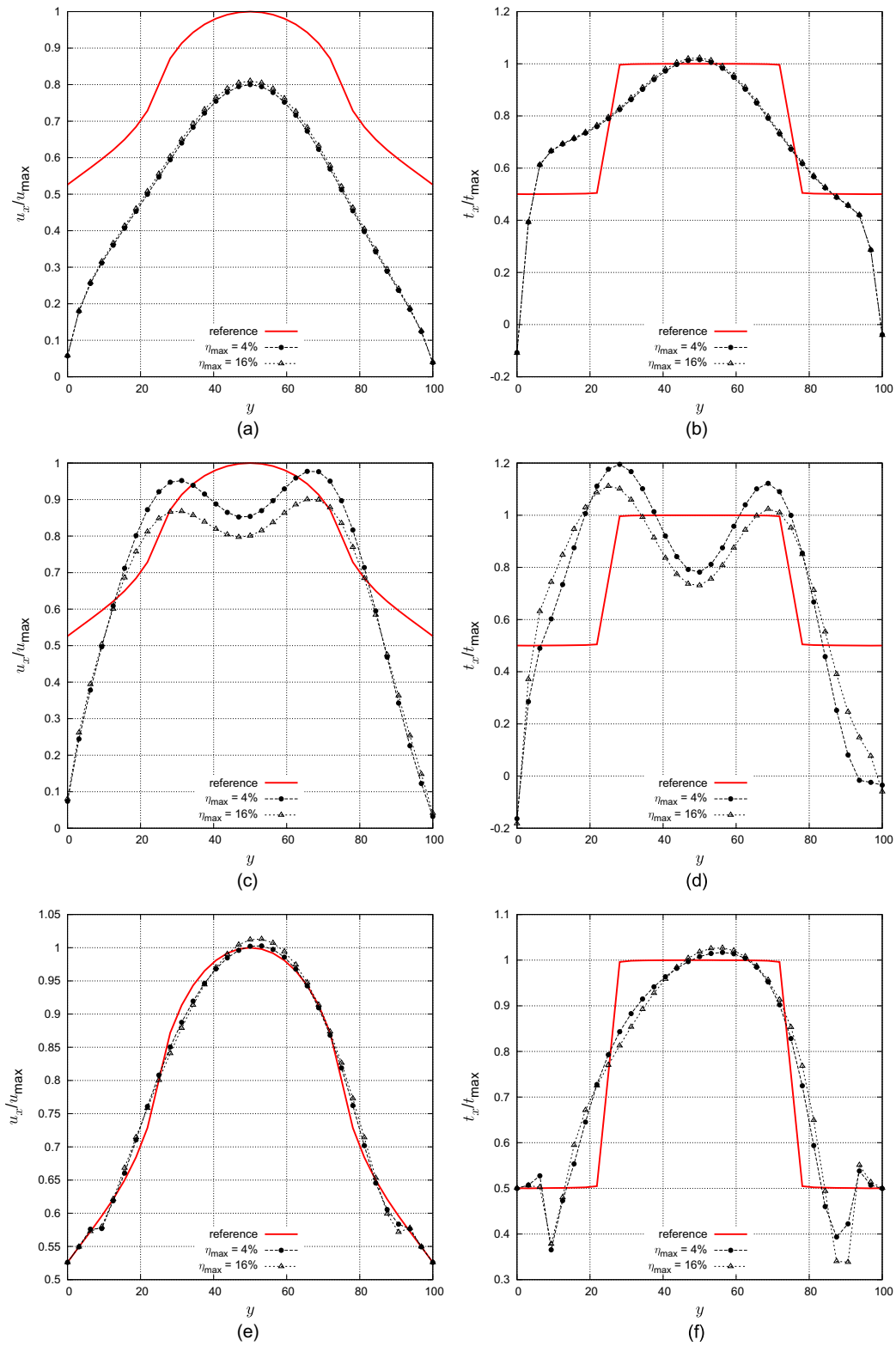

Fig. 25. Square plate stretched by discontinuous load: numerical results of the Cauchy problem compared with the reference solution for u_x (a, c, e) and t_x (b, d, f) on the side $x = -L/2$ noising tractions with $\eta_{\max} = 4\%,16\%$ for $\ell_o/\ell_u = 1/3$ (a, b), $\ell_o/\ell_u = 1$ (c, d), and $\ell_o/\ell_u = 3$ (e, f).

solution for u_x and t_x relative to the side $x = -L/2$ are reported on Fig. 25 where the boundary data are those already described in Table 2. These results are relative to the case of noise applied to the known traction with an error level of 4% and 16%. Analogous results are reported in Fig. 26 with the noise applied to the known displacements by using as error level 2% and 8%. In this case it is easy to observe that this kind of problem cannot be solved effectively by a regularizing approach which naturally tends to produce smooth solutions. However the main features of the boundary conditions to be reconstructed are captured.

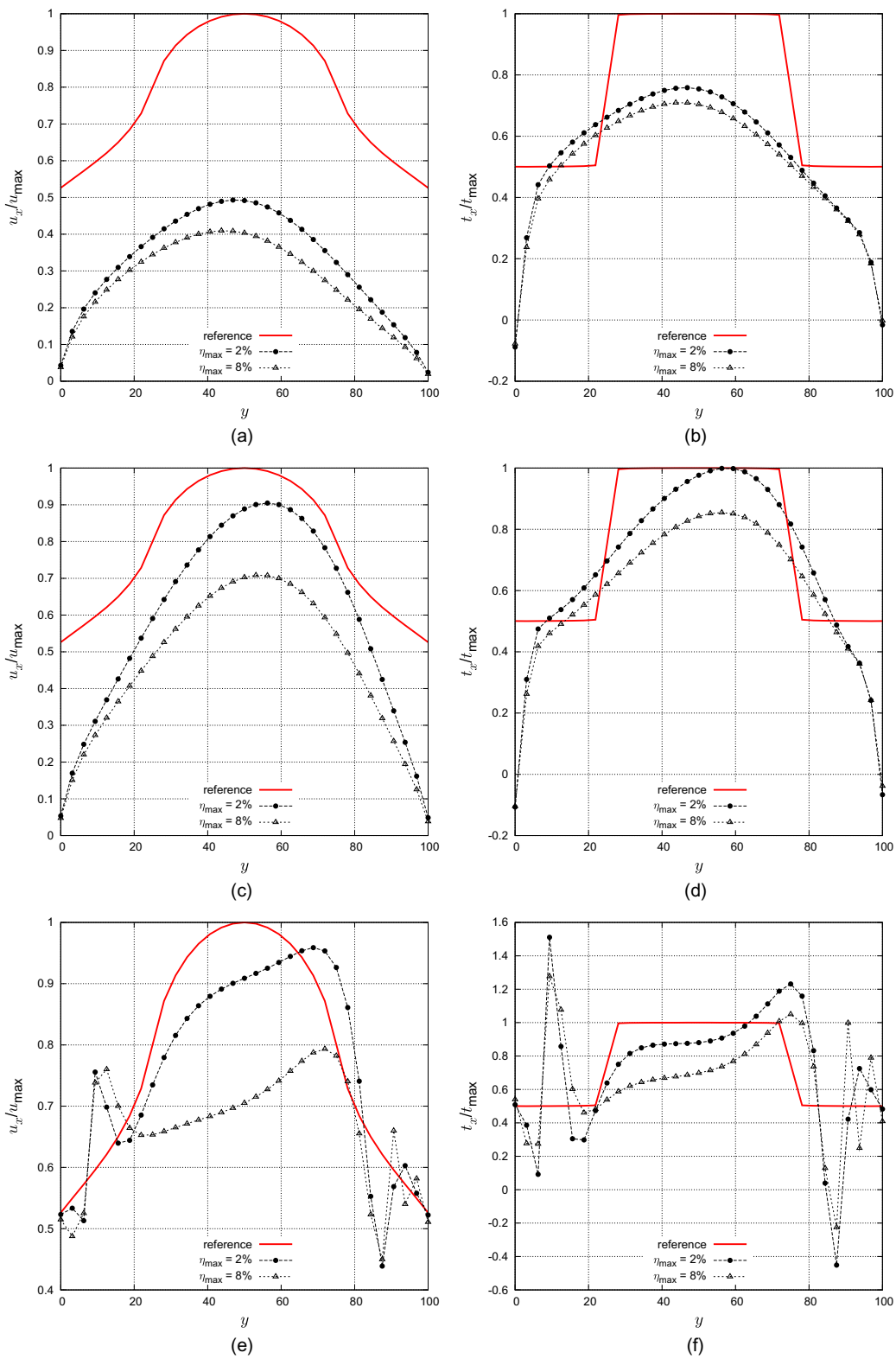

Fig. 26. Square plate stretched by discontinuous load: numerical results of the Cauchy problem compared with the reference solution for u_x (a, c, e) and t_x (b, d, f) on the side $x = -L/2$ noising displacements with $\eta_{max} = 2\%,8\%$ for $\ell_o/\ell_u = 1/3$ (a, b), $\ell_o/\ell_u = 1$ (c, d), and $\ell_o/\ell_u = 3$ (e, f).

5. Concluding remarks

A numerical experimentation regarding the solution of the Cauchy problem in two-dimensional linear elasticity has been discussed. Numerical results were obtained inside the frame of the regularization approach proposed by Tikhonov. This method stabilizes the least square method using a penalty term affected by a regularization parameter which balances the weight between problem equations and the *a priori* information on the solution. The optimal value of the regularization parameter was selected by using the Generalized Cross Validation criterion. The numerical tests were selected aiming at highlight the sensitivity of the solution with respect to the amount of Cauchy data available to solve the problem, data noise level, regularity of the boundary conditions and the regularization parameter.

On the basis of the numerical experimentation here presented the following remarks can be deduced.

1. The amount of Cauchy data available to solve the problem and also their position with respect to the boundary data to be identified have a significant impact over the quality of the obtained solution. In particular the increase of the ratio ℓ_o/ℓ_u, the length of the overdetermined part of the boundary over the length of the underdetermined part, allows to obtain a better solution along the underdetermined part of the boundary, in term of both displacements and tractions; in the case of the hollow cylinder a greater distance between the internal and external boundary improves the solution; for the square plate changing the overdetermined sides, without varying the ratio ℓ_o/ℓ_u, also affects the solution.
2. The perturbation of the Cauchy data influences, as expected, the solution, however the effect is very different if the perturbation is applied to the known traction or to known displacements. In all the tests considered the perturbation of the displacements has a strong effect and a significant difference can be observed for different values of the noise level. On the contrary the perturbation of the applied traction has minor effects and very slight differences can be noticed for different values of the noise level.
3. Filtering the errors which certainly affect data is a central point. In this case there are three aspects that must be considered: the functional to minimize, the *a priori* information on the solution and finally, but not less important, the choice of the optimal regularization parameter. In this work, we have used standard methods: least square for the functional to minimize, minimum norm bound on the solution for the *a priori* information and the Generalized Cross Validation criterion to select the optimal regularization parameter. Probably, the weak point of the chain is the bound on the solution. Minimum norm bound is adapt to select smooth solution but, obviously, its effectiveness is limited when discontinuous boundary conditions have to be reconstructed.
4. In the case of no error in the data the ill-conditioning of the algebraic system of equations can be circumvented by using a fixed value of the regularization parameter which allows to simply filter out roundoff errors. In this case the accuracy of the solution is comparable to that given by the solution of direct problem. However too refined meshes should be avoided because the intrinsic instability of the Cauchy problem could be triggered by the large number of unknowns.
5. The choice of the regularization parameter is a key-point for solving the ill-conditioned system of equations. A low sensitivity of the reconstruction error to this parameter in a large subset, as observed for the higher values of the ratio ℓ_o/ℓ_u, allows a pain-less choice of this parameter.

Finally, we list some open questions that, in our opinion, deserve an answer.

1. Discontinuous boundary conditions require a specific treatment, probably a stabilizing term that enclose the peculiarity of the boundary conditions to reconstruct could produce more accurate numerical results.
2. Error modeling is another aspect which deserves an adequate investigation in order to design realistic numerical models.
3. In this work the optimal regularization parameter was chosen by means of Generalized Cross Validation criterion which, in general, produces accurate results, however there are various other criteria that could be experienced or, in alternative, methods that does not requires a selection criterion (Cimetière et al., 2001).
4. Alternative minimum condition to solve the Cauchy problem could be used such as the minimization of the reciprocity gap as proposed in Bonnet and Constantinescu (2005).

References

Alessandrini, G., Morassi, A., Rosset, E., 2003. Size estimates. In: Alessandrini, G., Uhlmann, G. (Eds.), Inverse Problems: Theory and Applications. Contemporary Mathemathics. American Mathematical Society, Providence. pp. 1–33.

Alessandrini, G., Bilotta, A., Formica, G., Morassi, A., Rosset, E., Turco, E., 2005. Numerical size estimates of inclusions in elastic bodies. Inverse Problems 21, 133–151.

Andrieux, S., Baranger, T.N., 2008. An energy error-based method for the resolution of the Cauchy problem in 3D linear elasticity. Computer Methods in Applied Mechanics and Engineering 197, 902–920.

Andrieux, S., Baranger, T.N., Ben Abda, A., 2006. Solving Cauchy problems by minimizing an energy-like functional. Inverse Problems 22, 115–133.

Bastay, G., Kozlov, V.A., Turesson, B., 2001. Iterative methods for an inverse heat conduction problem. Journal of Inverse and Ill-Posed Problems 9, 375–388.

Bastay, G., Johansson, T., Kozlov, V.A., Lesnic, D., 2006. An alternating method for the stationary Stokes system. ZAMM-Zeitschrift für Angewandte Mathematik und Mechanik 86, 268–280.

Belgacem, F.B., 2007. Why is the Cauchy problem severely ill-posed? Inverse Problems 23, 823–836.

Bonnet, M., Constantinescu, A., 2005. Inverse problems in elasticity. Inverse Problems 21, 1–50.

Bourgeois, L., 2005. A mixed formulation of quasi-reversibility to solve the Cauchy problem for Laplace's equation. Inverse Problems 21, 1087–1104.

Braess, D., 1997. Finite Elements. Cambridge University Press.

Burke, B.C.P., Kim, S.O., Kim, K.S., 2007. Partial polar decomposition inverse method applied to determination of internal stresses in an elastic complex structures. International Journal of Solids and Structures 44, 2010–2020.

Cimetière, A., Delvare, F., Jaoua, M., Pons, F., 2001. Solution of the Cauchy problem using iterated Tikhonov regularization. Inverse Problems 17, 553–570.

Comino, L., Marin, L., Gallego, R., 2007. An alternating iterative algorithm for the Cauchy problem in anisotropic elasticity. Engineering Analysis with Boundary Elements 31, 667–682.

Golub, G.H., Van Loan, C.F., 1996. Matrix Computations, third ed. The Johns Hopkins University Press, Baltimore and London.

Golub, G.H., Health, M., Wahba, G., 1979. Generalized cross-validation as a method for choosing a good ridge parameter. Technometrics 21, 215–223.

Hansen, P.C., 1992. Numerical tools for analysis and solution of Fredholm integral equations of the first kind. Inverse Problems 8, 849–872.

Hào, D.N., Lesnic, D., 2000. The Cauchy problem for the Laplace's equation via the conjugate gradient method. IMA Journal of Applied Mechanics 65, 199–217.

Johansson, T., Lesnic, D., 2006a. A variational conjugate gradient method for determining the fluid velocity of a slow viscous flow. Applicable Analysis 85, 1327–1341.

Johansson, T., Lesnic, D., 2006b. Reconstruction of a stationary flow from incomplete boundary data using iterative methods. European Journal of Applied Mathematics 17, 651–663.

Johansson, T., Lesnic, D., 2007. An iterative method for the reconstruction of a stationary flow. Numerical Methods for Partial Differential Equations 23, 998–1017.

Jourhmane, M., Lesnic, D., Mera, N.S., 2004. Relaxation procedures for an iterative algorithm for solving the Cauchy problem for the Laplace equation. Engineering Analysis with Boundary Elements 28 (6), 655–665.

Kaipio, J.P., Somersalo, E., 2004. Statistical and Computational Inverse Problems. Springer.

Klibanov, M.V., Santosa, F., 1991. A computational quasi-reversibility method for Cauchy problems for Laplace's equation. SIAM Journal on Applied Mathematics 51 (6), 1653–1675.

Koya, T., Yeih, W.C., Mura, T., 1993. An inverse problem in elasticity with partially overspecified boundary conditions. II. Numerical details. Transactions of the ASME Journal of Applied Mechanics 60, 591–606.
Kozlov, V.A., Maz'ya, V.G., Fomin, A.F., 1991. An iterative method for solving the Cauchy problem for elliptic equations. Computational Mathematics and Mathematical Physics 31 (1), 45–52.
Lattès, R., Lions, J.L., 1967. Méthode de quasi-réversibilité et applications. Dunod.
Lesnic, D., Elliot, L., Ingham, D.B., 1997. An iterative boundary element method for solving the Cauchy problem for the Laplace equations. Engineering Analysis with Boundary Elements 20, 123–133.
Maniatty, A.M., Zabaras, N.J., 1994. Investigation of regularization parameters and error estimating in inverse elasticity problems. International Journal for Numerical Methods in Engineering 37, 1039–1052.
Maniatty, A.M., Zabaras, N.J., Stelson, K., 1989. Finite element analysis of some elasticity problems. Journal of Mechanical Engineering Division ASCE 115, 1302–1316.
Marin, L., 2005. A meshless method for solving the Cauchy problem in three-dimensional elastostatics. Computers & Mathematics with Applications 50, 73–92.
Marin, L., 2009a. The minimal error method for the Cauchy problem in linear elasticity. Numerical implementation for two-dimensional homogeneous isotropic linear elasticity. International Journal of Solids and Structures 46, 957–974.
Marin, L., 2009b. Boundary element-minimal error method for the Cauchy problem associated with Helmholtz-type equations. Computational Mechanics 44, 205–219.
Marin, L., Lesnic, D., 2002a. Boundary element solution for the Cauchy problem in linear elasticity using singular value decomposition. Computer Methods in Applied Mechanics and Engineering 191, 3257–3270.
Marin, L., Lesnic, D., 2002b. Regularized boundary element solution for an inverse boundary value problem in linear elasticity. Communications in Numerical Methods in Engineering 18, 817–825.
Marin, L., Lesnic, D., 2003. BEM first-order regularization method in linear elasticity for boundary identification. Computer Methods in Applied Mechanics and Engineering 192, 2059–2071.
Marin, L., Lesnic, D., 2004. The method of fundamental solutions for the Cauchy problem in two-dimensional linear elasticity. International Journal of Solids and Structures 41, 3425–3438.
Marin, L., Lesnic, D., 2005. Boundary element-Landweber method for the Cauchy problem in linear elasticity. IMA Journal of Applied Mathematics 70, 323–340.
Marin, L., Elliot, L., Ingham, D.B., Lesnic, D., 2001. Boundary element method for the Cauchy problem in linear elasticity. Engineering Analysis with Boundary Elements 25 (9), 783–793.
Marin, L., Elliot, L., Ingham, D.B., Lesnic, D., 2002a. An iterative boundary element algorithm for a singular Cauchy problem in linear elasticity. Computational Mechanics 28, 479–488.
Marin, L., Hào, D.N., Lesnic, D., 2002b. Conjugate gradient-boundary element method for the Cauchy problem in elasticity. Quarterly Journal of Mechanics and Applied Mathematics 55, 227–247.
Marin, L., Elliot, L., Heggs, P.J., Ingham, D.B., Lesnic, D., Wen, X., 2003a. An alternating iterative algorithm for the Cauchy problem associated to the Helmholtz equation. Computer Methods in Applied Mechanics and Engineering 192, 709–722.
Marin, L., Elliot, L., Heggs, P.J., Ingham, D.B., Wen, X., 2003b. Conjugate gradient-boundary element solution to the Cauchy problem for the Helmholts-type equations. Computational Mechanics 31, 367–377.
Marin, L., Elliot, L., Heggs, P.J., Ingham, D.B., Lesnic, D., Wen, X., 2004a. BEM solution for the Cauchy problem associated with Helmholts-type equations by the Landweber method. Engineering Analysis with Boundary Elements 28, 1025–1034.
Marin, L., Elliot, L., Heggs, P.J., Ingham, D.B., Lesnic, D., Wen, X., 2004b. Comparison of regularization methods for solving the Cauchy problem associated with the Helmholtz equation. International Journal for Numerical Methods in Engineering 60, 1933–1947.
Schnur, D., Zabaras, N.J., 1990. Finite element solution of two-dimensional elastic problems using spatial smoothing. International Journal for Numerical Methods in Engineering 30, 57–75.
Tikhonov, A.N., Arsenin, V.Y., 1977. Solution of Ill-Posed Problems. John Wiley & Sons, New York.
Timoshenko, S.P., Goodier, J.N., 1970. Theory of Elasticity. McGraw-Hill International.
Turco, E., 1998. Load distribution modelling for pin-jointed trusses by an inverse approach. Computer Methods in Applied Mechanics and Engineering 165, 291–306.
Turco, E., 1999. A boundary elements approach to identify static boundary conditions in elastic solids from stresses at internal points. Inverse Problems in Engineering 7, 309–333.
Turco, E., 2001. An effective algorithm for reconstructing boundary conditions in elastic solids. Computer Methods in Applied Mechanics and Engineering 190, 3819–3829.
Wang, J., Sun, F.-Y., Jin, B.T., 2006. Method of fundamental solutions for a three-dimensional inverse problem in linear elasticity. Journal of Zhejiang University (Science Edition) 33, 134–138.
Yeih, W.C., Koya, T., Mura, T., 1993. An inverse problem in elasticity with partially overspecified boundary conditions. I. Theoretical approach. Transactions of the ASME Journal of Applied Mechanics 60, 595–600.
Zabaras, N.J., Morellas, V., Schnur, D., 1989. Spatially regularized solution of inverse elasticity problems using the BEM. Communications in Applied Numerical Methods 5, 547–553.
Zienkiewicz, O.C., Taylor, R.L., 2000. The Finite Element Method. Butterworth-Heinemann.